Dendritic Sensitivity to the Direction of Synaptic Firing Mediated by Inhibition

and

The Effects of the Release Timecourse of Neurotransmitter on Synaptic Transmission

by

Boris Krupa

B.Sc., Computer Science
B.A., Philosophy
University of Chicago, 2000

Submitted to the Department of Brain and Cognitive Sciences in Partial Fulfillment of the Requirements for the Degree of Doctor of Philosophy In Neuroscience

at the

Massachusetts Institute of Technology

February, 2006

Signature of Author:

Department of Brain and Cognitive Sciences
December 29, 2005

Certified by:

Guosong Liu
Associate Professor of Neurobiology
Thesis Supervisor

Accepted by:

Earl K. Miller
Picower Professor of Neuroscience
Chairman, Department Graduate Committee

TABLE OF CONTENTS

I. INTRODUCTION

This thesis contains two main projects that I worked on during my graduate studies at MIT. Both address the subject matter of how neurons communicate, process, and pass information within the context of larger neuronal ensembles.

The first project focuses on information transfer between two neurons during synaptic transmission. The project was spurred by an initial observation that neuronal communication through synapses in young and developing neuronal networks is only "half-hearted" in that signals propagate predominantly through only one type of synaptic receptor (the NMDA receptor), and bypass the principal signaling pathway present in mature synaptic transmission (AMPA receptor) (Malenka and Nicoll 1997). The possible cause of this abnormality was either that AMPA receptors were lacking on the postsynaptic side, or that something else in the process of synaptic transmission rendered them inoperable. The initial experiments in our laboratory established that this type of "incomplete" signaling within a synapse might be caused by a slowed release of neurotransmitter from the presynaptic vesicles (Renger, Egles et al. 2001). These initial experiments prompted a more complete investigation of the effects of the timecourse of neurotransmitter release from vesicles on the activation of synaptic receptors during synaptic transmission. Using focal application of neurotransmitter with high spatial and temporal resolution to target individual synapses, a technique perfected in our laboratory, we applied neurotransmitter transients with different temporal profiles to synaptic receptors and investigated their effects on the magnitude of the receptor's response. We found that a large fraction of synaptic receptors (namely, the receptors with slow >5 ms kinetics) were insensitive to the particular profile of neurotransmitter delivery. However, receptors with fast kinetics were sensitive to changes in the timecourse of neurotransmitter release, to the point that they would not pass any currents during slow neurotransmitter discharge (>5 ms) hypothesized to occur in immature synapses. The goal of the project was then to completely characterize the dependency of the receptor response on the timecourse of neurotransmitter delivery. This goal was achieved

and the results are presented in Chapter II of the thesis. The experiments presented help elucidate the effects of various presynaptic factors that affect the timecourse of neurotransmitter release on the fidelity of synaptic transmission.

The next project addressed a classic problem from neural information processing – how does the brain recognize and discriminate temporal sequences of events? That particular cells in the brain are capable of this computation has been long known. For instance, firing of retinal ganglion cells exhibits sensitivity to the direction of motion of a light stimulus on the retina (Taylor, He et al. 2000; Euler, Detwiler et al. 2002; Fried, Munch et al. 2002), a simplest form of spatio-temporal sequence. In the visual cortex, simple cells have been shown to display an analogous sensitivity to the direction of light motion (Borg-Graham, Monier et al. 1998; Anderson, Binzegger et al. 1999; Priebe and Ferster 2005). Likewise, in the hippocampus, a portion of cells has been shown to be sensitive to the direction of a rat's motion on a linear track (Wilson and McNaughton 1993; Frank, Brown et al. 2001). The neural correlate of such motion at a neural population level is a distinct temporal sequence of activation of the simple hippocampal place cells; however, some cells have been shown to be able to discriminate such population code, and respond preferentially to a rat's movement and progression in a particular direction, versus the opposite.

The question is whether the computation that recognizes a particular sequence of neuronal activity and prefers it over another sequence requires a large network for its instantiation, or whether it can be computed at the level of an individual neuron. Numerous proposals for the computation at the level of an individual cell have been put forth. The leading theory proposed that it could be instantiated by specific interplay between excitatory and inhibitory connections at the level of individual dendrites (Koch, Poggio et al. 1983; Grzywacz and Koch 1987). While the theory is reasonable, its plausibility has never been tested by experiment. I set out to investigate this question by carefully examining the functional interactions between excitatory and inhibitory connections on the dendrite, and their effect on the output of the cell.

The simplest temporal sequence is comprised of two inputs whose relative order and timing may vary. Using focal application of excitatory and inhibitory neurotransmitters to individual synaptic loci on the dendrite, I therefore investigated the effects of the timing and location of 1) two excitatory synapses and 2) an excitatory and an inhibitory synapse on the magnitude of the neuronal response. The relative order of firing and the position of two excitatory inputs turned out to be generally irrelevant to the magnitude of the neuronal response. Thus, excitation alone could not be solely responsible for sequence discrimination. However, when excitation was coupled to inhibition, a strong temporal and spatial asymmetry in the activation function arose. Only when inhibition preceded excitation, but not vice versa, the response of the neuron was cancelled out. Spatially, only if inhibition lied "on the path" between the excitatory input and the cell body, but not further from the cell, the neuronal response vanished. These observations are consistent with the assumptions of the theory of Koch et al. predicting dendritic directional selectivity. I therefore further investigated the possibility that these asymmetric interactions might confer directional sensitivity to the dendrite, and the ability to discriminate particular sequences of activation of its inputs. To do this, I stimulated the synapses on the dendrite sequentially, using a customized software and a visual feedback for the micromanipulators used for neurotransmitter delivery.

The experiments presented in Chapter III represent the first experimental verification of the hypothesis raised more than two decades ago that nonlinearity of shunting inhibition might confer direction sensitivity to dendrites (Koch, Poggio et al. 1983; Grzywacz and Koch 1987). I further investigated the implications of this nonlinear interaction for coding of temporal sequences. Based on some general considerations of the economy of synaptic wiring in the brain, I find that such directional sensitivity might result in the sensitivity of neurons in a two-dimensional neural sheet (such as the surface of the cortex) to the direction of activation of other neurons.

Both Chapter II and Chapter III are written in a form suitable for publication in a scientific journal. The publication of both projects is actively pursued.

II. THE EFFECTS OF THE RELEASE TIMECOURSE OF NEUROTRANSMITTER ON RECEPTOR ACTIVATION

SUMMARY

The release mode of presynaptic neurotransmitter through the fusion pore has been suggested as a possible locus for the regulation of synaptic efficacy. It is therefore important to understand how different modes of presynaptic neurotransmitter release might affect activation of different postsynaptic receptor types. To address this question experimentally, we investigated the effects of the timecourse of fast ejections of fixed neurotransmitter packets on the response magnitude of three major postsynaptic receptor types. We found that receptors differed markedly in their sensitivities to the timecourse of neurotransmitter delivery. While the response of NMDA receptors was virtually insensitive to the temporal aspects of delivery, as long as the amount of neurotransmitter was conserved, the peak responses of AMPA and $GABA_A$ receptors to fixed neurotransmitter packets depended strikingly on the speed of release, with slow ejections eliciting markedly smaller response compared to the magnitude elicited by near instantaneous release. We examined a number of release paradigms and multiple contents of the released packets and found an equation that could closely predict the obtained response magnitudes over a wide range of release parameters. This equation predicts that the magnitude of the receptor response during brief neurotransmitter release episodes depends on only three factors - the total vesicular content of neurotransmitter downscaled by the diffusional distance, the duration of the release pulse relative to the decay time constant of the receptor current, and the binding rate between the receptor and the agonist. These three factors quantitatively predict the magnitude of the receptor currents over a wide range of neurotransmitter delivery paradigms and over six synaptic receptor types, and can therefore serve as a unified basis for understanding the

effects of presynaptic release profiles, caused by different kinetics of fusion pore opening, on receptor activation.

INTRODUCTION

Quantal synaptic transmission is the elementary unit of neural communication. The strength of quantal synaptic transmission depends on several factors: the presynaptic release of neurotransmitters, their diffusion through the synaptic cleft, and, ultimately, binding and gating of the postsynaptic receptor channels. To understand how the postsynaptic response is generated, it is therefore necessary to understand how these three processes interact. All three processes of synaptic transmission have been studied extensively in isolation (Colquhoun, Jonas et al. 1992; Edmonds, Gibb et al. 1995; Sakmann and Neher 1995; Clements 1996; Zucker 1996; Rizo and Sudhof 2002). However, how different aspects of presynaptic release, such as the rate of neurotransmitter release, the number of released neurotransmitter molecules, or the particular time course of neurotransmitter generated in the synaptic cleft affect receptor activation in the endogenous context of synaptic transmission is still a subject of active research (for recent reviews see Liu 2003; Stevens 2003).

For instance, it has been recently hypothesized that different rates of neurotransmitter release from presynaptic vesicles might affect the magnitude of the postsynaptic receptor currents at CNS synapses (for recent reviews see Choi, Klingauf et al. 2003; Krupa and Liu 2004). Along this line of reasoning, a switch in the mode of neurotransmitter release during neural development has been suggested to turn on "silent" synapses, which are characterized by the absence of AMPA receptor (AMPAR) currents, into functional ones, containing a pronounced AMPAR component. Traditionally, the absence of AMPAR currents has been interpreted by the lack of postsynaptic AMPA receptors in the synapse (Isaac, Nicoll et al. 1995; Liao, Hessler et al. 1995). However, the observation that slow mode of glutamate release might selectively activate NMDA receptors

without activating AMPA receptors provided an alternative presynaptic mechanism (Choi, Klingauf et al. 2000; Renger, Egles et al. 2001). Today multiple lines of evidence lend credence to the possibility that AMPAR-free synaptic transmission might be in some cases generated by slow neurotransmitter discharge from vesicles. First, increase in the rate-of-rise and peak of glutamate in the synaptic cleft accompanies LTP at young hippocampal neurons (Choi, Klingauf et al. 2000), suggesting that presynaptic release of glutamate is accelerated during the augmentation of AMPAR-mediated synaptic currents. Second, a direct interference with the presynaptic vesicle fusion machinery can selectively disrupt AMPA receptor-mediated transmission, without disrupting signaling through the NMDA receptors (Renger, Egles et al. 2001). Third, terminals in hippocampal slices lose their ability to release but not take up fluorescent dyes after LTD, advocating the possibility that LTD mediates a switch in the dynamics of fusion pore opening (Zakharenko, Zablow et al. 2001; Zakharenko, Zablow et al. 2002). Based on these reports, it became increasingly important to understand how the dynamics of presynaptic neurotransmitter flux affects the activation of different postsynaptic receptors.

The problem of how the dynamics of neurotransmitter release from presynaptic vesicles affects receptor activation is an instance of a more general problem – how is receptor signaling affected by the timecourse of neurotransmitter in the synaptic cleft? Apart from the rate of neurotransmitter release through the fusion pore, cleft timecourse of neurotransmitter might also be influenced by factors such as the alignment of the vesicle fusion site relative to the postsynaptic receptor cluster (Franks, Stevens et al. 2003), the general morphology of the synapse, the rate of neurotransmitter diffusion (Clements 1996; Min, Rusakov et al. 1998) and/or neurotransmitter reuptake and enzymatic degradation (Isaacson and Nicoll 1993; Tong and Jahr 1994; Kidd and Isaac 2000). The effects of neurotransmitter timecourse on receptor activation have been previously studied experimentally (Clements, Lester et al. 1992; Colquhoun, Jonas et al. 1992; Tong and Jahr 1994; Jones, Sahara et al. 1998; Chen, Ren et al. 2001), but these studies have been largely qualitative and did not provide quantitative predictions about the receptor response to different temporal neurotransmitter profiles. At the other extreme, the problem can be

attacked with detailed simulations (Franks, Bartol et al. 2002), but simulations, albeit highly quantitative, do not provide a simple insight into the critical parameters that determine the degree of receptor response to brief neurotransmitter pulses. Thus, as a more general problem, we sought a simple quantitative understanding of how the timecourse of neurotransmitter within synaptic cleft interacts with different receptor properties and determines the magnitude of their response.

In order to study the effects of different release dynamics of neurotransmitter from vesicles on the activation of different postsynaptic receptors, we attempted to mimic the process of vesicular neurotransmitter release with different dynamics by administering short iontophoretic pulses of neurotransmitter to AMPA, NMDA, and $GABA_A$ receptors located in outside-out patches and intact synapses. We found that the receptors responded differently to different temporal delivery profiles of neurotransmitter. Whereas NMDA receptors were virtually unaffected by the timecourse of neurotransmitter delivery up to 16 ms pulse durations, AMPA and $GABA_A$ receptors were activated only partially during slower neurotransmitter ejections. We searched for a general scheme that would predict the magnitude of the receptor responses during fast neurotransmitter applications and found that an equation based on only three receptor properties could adequately describe the response magnitudes of all three studied receptor species. The generalizability of this equation to three other major ligand-gated receptors was further tested in simulations. Thus, a single and relatively simple formalism can be used to predict the response magnitude of six major fast synaptic receptor types to fast neurotransmitter fluxes, which aids better understanding of how the synaptic response is generated during quantal synaptic transmission. Finally, we discuss the possible effects of physiological modulations of the fusion pore-mediated dynamics of neurotransmitter release on the activation of various synaptic receptor types.

RESULTS

To study the effects of different dynamics of neurotransmitter discharge from vesicles on receptor activation, we sought a way of experimentally mimicking the process of neurotransmitter flux via fusion pores with different properties (conductance, open time, etc.). This required a way of delivering a fixed amount of neurotransmitter to receptors with different temporal profiles. We therefore chose the technique of neurotransmitter delivery by iontophoresis, in which the number of ejected molecules is directly proportional to the total delivered electric charge (Dionne and Stevens 1975; Trussell, Thio et al. 1988; Murnick, Dube et al. 2002), while the rate of neurotransmitter delivery can be controlled by the magnitude of the applied current. As iontophoresis traditionally suffered form the lack of adequate spatial and temporal precision to mimic neurotransmitter release from vesicles, we used an improved iontophoresis system capable of ejecting neurotransmitter on a sub-millisecond timescale and localizing the release pulse to individual synapses (Murnick, Dube et al. 2002). Fig. 1A shows the micropipette used for neurotransmitter delivery positioned over a single synapse (green) from a cultured hippocampal neuron. To verify the capability of the iontophoresis system to deliver a designated concentration profile of neurotransmitter to the receptors, we measured the concentration of the Oregon Green fluorescent dye ejected from the pipette at 0.5 μm distance from the electrode tip (a typical distance between the receptor patch and the electrode tip in subsequent experiments) in response to a family of ejection currents of various durations and amplitudes (Fig. 1B-C). We used fluorescence measurements because it was otherwise impossible to measure the neurotransmitter concentration directly. The amount of neurotransmitter ejected by the device scaled linearly with the magnitude and the duration of the applied current (Fig. 1B-C; inset). Furthermore, the obtained fluorescence data could be fitted by the point-source diffusion equation, shown as smooth lines in Figs. 1B-C (see Methods). We therefore concluded that the device allowed for a linear control of neurotransmitter delivery; and the concentration profile obeyed the point-source diffusion law for ejections as short as 0.5 ms. This permitted us to estimate the concentration profile of the released neurotransmitter at 0.5 μm distance from

the electrode tip by substituting the diffusion constant of the neurotransmitter (D_{glut} ~ 0.75 $\mu m^2/ms$; D_{GABA} ~ 0.83 $\mu m^2/ms$) for that of Oregon Green (D ~ 0.53 $\mu m^2/ms$) in the diffusion equation **(2)**. Fig. 1D displays the calculated transmitter concentrations in response to a family of command pulses that preserved the amount of released molecules, and changed only the release dynamics. Note that the areas under the concentration curves are equal (since the number of neurotransmitter molecules was preserved), but the estimated peak concentrations vary 3-fold between the release durations of 0.5 and 2 ms. Thus, the rate of neurotransmitter release from the iontophoresis electrode had a significant effect on the timecourse of neurotransmitter at the receptors at 0.5 μm distance.

Despite our efforts to speed up the neurotransmitter delivery system, the generated concentration waveforms were still an order of magnitude slower and blunter than the timecourse generated by neurotransmitter release from vesicles at mature synapses (less than ~100 μs (Almers, Breckenridge et al. 1991; Stiles, Van Helden et al. 1996)). However, the resolution of our technique might be adequate for mimicking neurotransmitter release at "silent" synapses. For instance, Choi et al. report synaptic currents with slow rise-times of 4.1 ms recorded from silent synapses in hippocampal cultures, advocating presynaptic release within this timescale (Choi, Klingauf et al. 2000). Recently, neurotransmitter release from the microvesicles of the posterior pituitary gland with low fusion pore conductance of 19 pS has been estimated to last as long as 5 ms (Klyachko and Jackson 2002). The iontophoresis system might therefore be adequate for examining the possible effects of a slowed down presynaptic release, such as through a low conducting or slowly-dilating fusion pore (Choi, Klingauf et al. 2000; Renger, Egles et al. 2001; Klyachko and Jackson 2002). The concentration waveforms generated by iontophoresis are comparable to those generated at the synapse by slowly releasing vesicles (Fig. 1D; inset). Finally, the behavior of the receptors during shorter release intervals than those tested (< 0.5 ms duration) can be in principle inferred by extrapolation from the response to the shortest tested (0.5 ms) ejection pulses.

THE EFFECTS OF THE TIMECOURSE OF NEUROTRANSMITTER DELIVERY ON RECEPTOR ACTIVATION

The basic effect of the timecourse of neurotransmitter delivery on receptor activation is shown in Fig. 2. Here, a fixed amount of neurotransmitter (64 pC iontophoretic charge) was iontophoretically applied at various rates to receptors located in an outside-out patch positioned as close as possible to the iontophoresis electrode tip (typically within 0.5 μm distance, inspected visually). The amount of released neurotransmitter was constrained to prevent receptor saturation (64 pC iontophoretic pulse evoked ~75% receptor occupancy). We found that AMPA and $GABA_A$ receptors were very sensitive to the timecourse of neurotransmitter delivery. The $GABA_A$ receptor peaks diminished by more than 50% in response to 16 ms versus 0.5 ms ejections of the same neurotransmitter content, and AMPA receptor responses to 16 ms ejections vanished almost entirely. By contrast, NMDA receptors were largely insensitive to the temporal profile of glutamate delivery; the receptor currents had equal shapes and magnitudes despite more than 20-fold difference in the peak concentration of glutamate at the receptors (calculated as in Fig. 1D). These data suggest that AMPA and $GABA_A$ receptors but not NMDA receptors are strongly influenced by the temporal profile of neurotransmitter release.

To explore this phenomenon more systematically, we methodically varied the rate and the duration of glutamate flux applied to NMDA receptors first in outside-out patches. Pulse durations ranged from 0.5 ms to 16 ms and the rate was scaled such that the total amount of ejected neurotransmitter was preserved (shown as traces of equal color; Fig. 3A). The recorded NMDA receptor currents are shown in Fig. 3A. We observed that the peak responses of the NMDA receptors to glutamate pulses of different durations but equal glutamate content appeared almost identical across a wide range of applied glutamate amounts (Fig. 3B; $p > 0.99$ for independence of the response peak on the ejection interval, one-way ANOVA). The slight attenuation of the receptor peak response to very long and low iontophoretic currents can be attributed to the sub-optimal ejection properties of the iontophoresis device at command currents below 2 nA (see Methods).

As the magnitude of receptor response is classically understood in terms of the ligand concentration and its affinity for the receptor, we wanted to test whether the peak receptor currents correlated with the peak concentration of glutamate generated at the receptors. We therefore analyzed the peak receptor response as a function of the peak glutamate concentration (Fig. 3C). We found that the concentration dependent dose-response curves shifted according to the duration of the ejection pulse. Thus, the peak concentration of agonist at the receptors alone was not a good predictor of their response magnitudes. This is in agreement with previous observations (Perkel and Nicoll 1993; Tong and Jahr 1994; Holmes 1995; Chen, Ren et al. 2001). However, we found that the NMDA receptor peak currents could be predicted accurately from the integral of the neurotransmitter timecourse passing the receptors, which, under constant geometry, is proportional to the ejected glutamate amount and independent of ejection timecourse (Fig. 3D, χ^2/d.o.f. = 0.15; $p > 0.99$). We therefore concluded that the NMDA receptors behaved as molecular *integrators* of the applied neurotransmitter, in that their activation up to 16 ms neurotransmitter pulses depended only on the total amount of glutamate passing the receptor (proportional to the amount released), but did not depend on the application rate or the peak agonist concentration alone.

We next studied the activation properties of AMPA and $GABA_A$ receptors, in response to the same stimulation protocol (glutamate was replaced with GABA in the study of $GABA_A$ receptors). Again, we analyzed the peak receptor currents as a function of the ejection pulse duration (Fig. 4). Although both AMPA and $GABA_A$ receptors responded similarly to pulses of equal agonist content applied rapidly (< 2 ms), both receptors showed a significant decrease in peak response to more prolonged ejections. Thus, in contrast with the NMDA receptors, AMPA and $GABA_A$ receptors appeared to behave as *leaky* integrators of the neurotransmitter, in that their peak response during longer neurotransmitter pulses was significantly attenuated relative to the peak response to an instantaneous transmitter application. To quantify the degree of the receptors' inability to respond to slower ejections of equal agonist amount, we fitted the evoked receptor current peaks approximately as an

exponential function of the agonist application interval (see below and Methods for the fitting equation) and noted the corresponding exponential time constant. As this time constant denotes the receptors' ability to integrate and respond to different rates of delivery of a constant neurotransmitter amount, we called it the receptor integration time constant τ_{int}. The τ_{int} for the AMPA receptors was estimated as 2.6 ± 0.4 ms. The interpretation of this value is that the response of AMPA receptors to a small amount of glutamate released over 2.6 ms is e-fold smaller in magnitude than the response to the same glutamate amount released instantaneously. By contrast, the τ_{int} for GABA and NMDA receptors were estimated as 14.2 ± 2.4 ms and 64.0 ± 28.5 ms respectively. Thus, GABA receptors were better at responding to slowly released neurotransmitters (τ_{int} = 14.2 ± 2.4 ms) than AMPA receptors (τ_{int} = 2.6 ± 0.4 ms), and NMDA receptors were best at responding to slowly delivered agonist (τ_{int} = 64.0 ± 28.5 ms).

Next, to ensure that receptors at synapses exhibit similar behavior to the receptors in excised somatic patches studied above, we applied short agonist pulses to receptors located at synapses on the dendrites of cultured hippocampal neurons identified by the fluorescent marker FM1-43 (configuration shown in Fig. 1A). Although delivery of neurotransmitter by iontophoresis to receptors in an excised patch is fast enough to ensure millisecond-range transients, there are two potential problems with using iontophoresis to study the response properties of the receptors at synapses to brief neurotransmitter fluxes: 1) neurotransmitter has to diffuse into the synapse from the extracellular medium; this could potentially blunt and slow down the timecourse of neurotransmitter in the synapse versus that in the free medium, and 2) neurotransmitter might activate receptors located in adjacent synapses or receptors located in the perisynaptic region. However, these potential caveats should not affect the results. To addres the first issue, we had previously verified that iontophoretic delivery of neurotransmitter to synapses is capable of evoking synaptic AMPA receptor currents with ~0.65 ms 20-80% rise-time, which is comparable to the fastest endogenous rise time during spontaneous (miniature) release events (Murnick, Dube et al. 2002). This fast rise-time suggests that the neurotransmitter concentration transient in the synaptic cleft

is not smeared by diffusion from the extrasynaptic space beyond several hundred microseconds. Diffusion into synaptic cleft might therefore smear the transmitter timecourse in the synaptic cleft associated with the shortest ejection pulses (< 1ms) but not with longer transmitter ejections. To address the second issue, we have studied receptors located at FM-marked synapses separated by at least 8 μm. Since the iontophoresis technique achieves spatial precision of ~1-3 μm (Murnick, Dube et al. 2002), this ensured that iontophoresis did not stimulate multiple FM-positive synapses. Furthermore, the density of the receptors in the perisynaptic region immediately outside the FM-labeled puncta has been shown to be 100x lower than that of the receptors in the synaptic cleft (Malenka and Nicoll 1999; Cottrell, Dube et al. 2000; Malinow, Mainen et al. 2000). These two facts together strongly suggest that the contamination of our recordings by currents from the extrasynaptic receptors or adjacent synapses was minimal.

Fig. 5 shows the currents recorded from synaptic AMPA, NMDA and $GABA_A$ receptors. The results are similar to those recorded from the somatic receptors in outside-out patches. In particular, both NMDA and GABA synaptic receptors were capable of responding to relatively slow and long agonist ejections relative to the AMPA receptors, which were almost incapable of response to glutamate pulses longer than 4ms. Accordingly, the τ_{int} of synaptic AMPA and GABA receptors were analogous to the values from the excised patch: 6.1 ± 0.8 ms and 14.6 ± 3.7 ms. The τ_{int} of synaptic NMDA receptors did not converge because NMDA receptors in this case integrated the applied glutamate pulse almost perfectly, consistent with any value of τ_{int} > 100 ms. One difference between the somatic receptors and the synaptic receptors was that the synaptic AMPA receptors (τ_{int} = 6.1 ± 0.8) were slightly more capable of responding to prolonged transmitter applications than the somatic AMPA receptors in outside-out patches (τ_{int} = 2.6 ± 0.4). This is consistent with the fact that the receptors in synapses also exhibited slower dissociation/desensitization kinetics (τ_{deact} = 17.3 ms) compared to the receptors in the outside-out somatic patches (τ_{deact} = 6.3 ms), which would make them into better integrators of the released transmitter (see below).

QUANTITATIVE ANALYSIS OF THE RECEPTOR RESPONSE TO BRIEF PULSES OF AGONIST

Based on the above experiments, it appeared that despite differences in the kinetic activation models of the three receptors studied (Jonas, Major et al. 1993; Jones and Westbrook 1995; Chen, Ren et al. 2001), their responses to brief neurotransmitter transients shared a number of common characteristics: 1) during very brief applications (shorter than τ_{int}), their response was virtually insensitive to the application timecourse of neurotransmitter, and, 2) during longer applications (τ_{int} or longer), their integrative capacity diminished. The difference between the receptors seemed to be mostly in the critical interval over which they became more sensitive to the ejection timecourse (τ_{int}). To understand the reason for this common behavior, we analyzed the kinetic schemes of the three receptors and found that their peak response to brief neurotransmitter transients can be understood in terms of three major kinetic properties: (1) the binding rate between the receptor and the agonist k_1, (2) the deactivation time constant of the receptor τ_{deact}, and (3) the number of receptor subunits required to bind agonist before channel opening N (see Appendix). The peak receptor response can be predicted from these 3 receptor properties and the agonist concentration timecourse by the following equation:

$$I_{peak} = I_{\max} \underbrace{\left(1 - e^{-k_1 Q}\right)^N}_{I.} \underbrace{e^{-T/\tau}}_{II.} \qquad \tau = \left(1 + 0.32 k_1 Q\right)\tau_{\text{int}} \qquad (1)$$

Here, $Q = \int_0^\infty A(t)\,dt$ is the integral of the agonist concentration timecourse generated at the receptor, T is the pulse duration over which agonist is applied, I_{max} is a normalization term which corresponds to the single channel current and the number of receptors in the receptor patch, and τ_{int} is the receptor integration time constant, which is proportional to τ_{deact}.

According to equation (1), if the duration of the ejection pulse is much shorter than the receptor's integration time constant τ_{int} ($T/\tau_{int} \rightarrow 0$), the receptor's peak response can be approximated by

$$I_{peak} \approx I_{max}\left(1-e^{-k_1 Q}\right)^N$$

Importantly, the quantity Q depends on the amount of applied neurotransmitter Φ and the distance between the neurotransmitter source and the receptor R ($Q \propto \Phi/R$) but is independent of the timecourse of neurotransmitter delivery. Therefore, the peak receptor response during agonist applications shorter than τ_{int} is largely independent of the delivery timecourse of neurotransmitter. This matches qualitatively the observations in Figs. 3-5. However, if the interval over which the neurotransmitter amount Φ is applied approaches τ_{int}, the peak response of the receptor will diminish exponentially, according to the second term in the equation. The convenience of the formulation in equation (1) lies in the fact that it condenses the effects of the application timecourse of neurotransmitter into a single exponential term (II.), whereas the first term (I.) is timecourse-independent and depends on other factors, such as the amount of applied transmitter, diffusion distance, etc.

We found that equation (1) captures the behavior of all the receptors studied above (Figs. 3-5; goodness of fit reported in Fig. legends). Thus, although AMPA, NMDA, and GABA receptors follow different activation kinetics (Jonas, Major et al. 1993; Jones and Westbrook 1995; Chen, Ren et al. 2001), their activation during brief neurotransmitter pulses could be described by a relatively simple model, based on just three receptor properties. Such simple formulation has a trivial advantage over more complex kinetic descriptions in its simplicity and fostering of conceptual insight, even though this might come at the expense of accuracy. The available complex kinetic models of AMPA, NMDA, and $GABA_A$ receptors are comprised of a large number of kinetic rate constants, which preclude the insight into the critical kinetic parameters that dominate the magnitude of their response during brief neurotransmitter pulses. A formulation based on three receptor parameters has the possible disadvantage of being only approximate, but offers a simpler conceptual

understanding. By analogy, the description of receptor activation in equilibrium by the Hill equation provides a simple conceptual insight into the role of different reaction parameters (such as receptor affinity and agonist concentration) on the receptor response magnitude, although this description is also in some cases incomplete (Kenakin 1997). Similarly, equation (1) provides simple insight into how the three receptor properties interact with neurotransmitter to produce the response of a wide range of receptor types to short neurotransmitter transients.

To test whether the simple model of receptor response to brief agonist pulses in equation (1) can be generalized to other ionotropic receptors, we numerically simulated the responses of acetylcholine receptors (AChR), kainate receptors (GluR6), and serotonin receptors (5HT-3) to neurotransmitter concentration profiles mimicking those used in the previous experimental protocols (Fig. 6). The simulations were based on the published kinetic models for the receptors (see Fig. legend). Fig. 6 shows that, despite the differences in the specific kinetic models of the receptors, their activation still followed the description offered by equation (1) during short pulses. The numerical simulations indicate that acetylcholine receptors (τ_{int} = 3.9 ± 0.6 ms) are poor integrators like AMPA receptors, kainate receptors (τ_{int} = 6.9 ± 0.5) are worse than AMPA but better than $GABA_A$ receptors in their integrative capacity, and serotonin receptors (τ_{int} = 85.0 ± 8.5 ms) are comparable to NMDA receptors and virtually insensitive to the timecourse of neurotransmitter delivery from an isolated compartment.

RECEPTOR INTEGRATION DEPENDS ON ITS DEACTIVATION TIME CONSTANT

Kinetic analysis predicts that the ability of the receptor to respond to prolonged neurotransmitter flux (τ_{int}) should be proportional to its ability to "hold on" to the agonist before dissociation (see Appendix). The receptor's integrating ability (τ_{int}) should therefore be inversely proportional to the rate of agonist dissociation from the receptor. However,

receptor desensitization will also diminish receptor activation during long applications. The size of the receptor's response to a prolonged neurotransmitter pulse should therefore be inversely proportional to the combination of two factors: agonist dissociation and receptor desensitization. Thus, τ_{int} should be proportional to the receptor deactivation time constant (τ_{deact}), measured as the (major) decay time constant of the evoked receptor current, which depends on the effects of both dissociation and desensitization. This holds true in the simplest receptor kinetic schemes (see Appendix). To test this hypothesis, we compared the integration time constant (τ_{int}) with the deactivation time constant (τ_{deact}) obtained from several receptor species or from different subtypes of a single receptor type. For instance, the hippocampal pyramidal neurons typically express AMPA receptors subtypes containing the GluR2 subunit (Siegel, Janssen et al. 1995; Bolshakov and Buldakova 2001), characterized by low Ca^{2+} permeability and relatively slow decay times due to slow desensitization (Grosskreutz, Zoerner et al. 2003), whereas interneuron-expressed AMPA receptors typically lack the GluR2 subunit (Leranth, Szeidemann et al. 1996) and exhibit much faster decay times. Based on the different kinetics, these two populations of AMPA receptors should therefore differ in their responsiveness to prolonged neurotransmitter pulses. Fig. 7A shows the response to different ejection profiles of a fixed neurotransmitter amount (evoking ~70% receptor activation) recorded from AMPA receptors synaptically located on pyramidal neurons and interneurons. The AMPA receptors found on the pyramidal neuron exhibited a slower decay timecourse (τ_{deact} = 16.1 ± 0.1 ms) and integrated longer neurotransmitter ejections better (τ_{deact} = 14.1 ± 0.2 ms) than the fast receptors on the interneuron (τ_{deact} = 8.8 ± 0.1; τ_{int} = 6.3 ± 0.7 ms). Fig. 7B pools the τ_{int} and τ_{deact} from a number of neurons expressing a natural variation of AMPA receptor subtype composition, and shows that the two quantities are tightly correlated. To further test the dependency of the receptors' integrative abilities on desensitization, we blocked AMPA receptor desensitization by cyclothiazide (100 μM) in the interneuron synapse, and observed a 12-fold increase in the decay time (τ_{deact} = 104.9 ± 0.1 versus τ_{deact} = 8.8 ± 0.1 ms control) and a >5-fold increase in the receptors' integrating ability (τ_{int} = 34.1 ± 17 ms versus τ_{int} = 6.3 ± 0.7 ms

control). Thus, the ability of the receptors to respond to slow and prolonged ejections of neurotransmitter depends on both the rate of dissociation and desensitization, and is proportional to τ_{deact}.

Finally, we compared the τ_{int} and τ_{deact} across the different receptor types studied experimentally and by simulations (Fig. 7C). It is evident that τ_{int} and τ_{deact} are correlated across all receptors considered – AMPA, NMDA, $GABA_A$, kainate, AChR and $5HT_3$ – although the correlation is less pronounced than within a single receptor type (Fig. 7B). As a general principle, therefore, it can be concluded that a receptor's integration time constant (τ_{int}) is proportional to the (major) decay time constant of its current, but the precise value of τ_{int} cannot be simply predicted from receptor kinetics (the correlation between τ_{int} and τ_{deact} is not perfect), and, for any given receptor species, τ_{int} must be measured experimentally or with detailed simulations.

THE PRINCIPLE OF PRESYNAPTICALLY "SILENT" SYNAPTIC TRANSMISSION

What are the implications of the principle of receptor activation embodied in equation (1) to synaptic transmission? We focus on the co-activation of AMPA and NMDA receptors by fast glutamate transient, since the ratio of their currents is important in determining the plasticity of synapses (Malenka and Nicoll 1999; Malinow, Mainen et al. 2000). We studied the relative activation levels of AMPA and NMDA receptors evoked in a single outside-out patch by iontophoretic applications of 0.5 ms duration. Fig. 8A shows the normalized peak receptor currents. In particular, we found that both receptors were saturated by approximately equal amounts of neurotransmitter and required equal amounts for 50% activation. This is consistent with previous findings (Tong and Jahr 1994; McAllister and Stevens 2000). However, this behavior is in sharp contradiction with the behavior of AMPA and NMDA receptors in equilibrium, in which AMPA receptors require 100-fold higher concentrations of glutamate for activation than NMDA receptors, based on

their 100-fold lower equilibrium affinity to glutamate (Patneau and Mayer 1990). This discrepancy between AMPA and NMDA receptor activation in equilibrium and during fast neurotransmitter can be explained by equation (1), according to which, during short release durations ($T << \tau_{int}$), receptor activation depends largely in the binding rate k_1. Since both AMPA and NMDA receptors bind glutamate at similar rates (Jonas and Sakmann 1992; Chen, Ren et al. 2001), their activation by submillisecond release pulses of the same neurotransmitter content should be similar.

What happens to the AMPA/NMDA ratio as the neurotransmitter ejection pulse lengthens? Fig. 8B shows that, during medium length ejection pulses (~4 ms), AMPAR response is attenuated relative to that of the NMDA receptors, and finally, during very long ejections (~16 ms), the AMPAR component of the response disappears almost entirely, whereas the NMDAR component remains almost unchanged. This result suggests that, other than missing AMPA receptors from young synapses (Gomperts, Rao et al. 1998; Petralia, Esteban et al. 1999), failure to activate AMPA receptors during "silent" synaptic transmission can be caused by slow presynaptic release of neurotransmitter (Choi, Klingauf et al. 2000; Renger, Egles et al. 2001). In Fig. 8C we show an instance of "silent" synaptic transmission in our preparation – when glutamate that evokes 50% NMDAR activation is ejected within 0.5 ms, it evokes a marked AMPAR response. However, if it is ejected over 16 ms, the NMDAR response is not significantly reduced, but the response of the AMPA receptors disappears entirely.

DISCUSSION

We have studied the effects of different temporal profiles of neurotransmitter delivery on the activation of several major ionotropic receptor species. We found that the degree of activation of all studied ligand-gated receptors during fast neurotransmitter applications could be closely predicted by an equation based on three receptor properties, the binding rate of the agonist (k_1), the receptor's integration time constant (τ_{int}), and the

number of agonist molecules required for receptor activation (N), and followed a simple set of principles:

i. If neurotransmitter is released within an interval much shorter than the receptor's integration time constant τ_{int}, receptor response is independent of the timecourse of neurotransmitter delivery.

ii. If neurotransmitter is released within an interval shorter than the receptor's integration time constant τ_{int}, the degree of receptor activation depends on the binding rate of the receptor with the agonist rather than the receptor's equilibrium affinity for the neurotransmitter ligand, and on the integral of the neurotransmitter concentration timecourse rather than the peak concentration alone.

iii. During more prolonged ejections ($T > \tau_{int}$), the degree of receptor activation by a fixed amount of released neurotransmitter (Φ) declines with an exponential dependence on the release duration T, according to the ratio T/τ_{int}. The receptor's integration time constant τ_{int} is inversely proportional to the rate of agonist dissociation and receptor desensitization, and is roughly proportional to the deactivation time constant of the receptor current (τ_{deact}).

Our findings are in qualitative agreement with previous studies of receptor responses to short neurotransmitter pulses (Clements, Lester et al. 1992; Colquhoun, Jonas et al. 1992; Tong and Jahr 1994; Jones, Sahara et al. 1998; Chen, Ren et al. 2001). Tong and Jahr (1994) varied the duration of the receptor's exposure to a fixed transmitter concentration, and reported that receptor activation increased during longer agonist pulses. This is consistent with principle ii), according to which the degree of receptor activation during brief transmitter pulses depends on the integral of the concentration timecourse at the receptor, and therefore should increase with longer pulses durations T of a constant concentration A (as $Q = AT$). The converse of this observation is that higher transmitter concentrations should be required to saturate receptors during shorter transmitter pulses. Accordingly, Chen et al. (2001) recently reported an apparent reduction of NMDA receptor affinity to glutamate during short versus sustained glutamate applications. These studies did not

quantify the effects of neurotransmitter timecourse on the size of receptor response, such as equation (1) here, and the results therefore cannot be compared quantitatively. Equation (1) ties together these diverse observations in a simple and coherent quantitative framework.

Our findings are also in qualitative agreement with previous Monte Carlo simulations of the effects of vesicle release on AMPA/NMDA receptor activation at synapses (Choi, Klingauf et al. 2003) and of different rates of fusion pore dilation on the magnitude of synaptic receptor currents (Clements 1996).

Because the integration time constant of most receptors is longer than the typical time span of vesicle release (with the possible exception of AMPA and acetylcholine receptors during slow "silent" synaptic transmission), receptor activation during typical mature synaptic transmission should be understood in term of principles i) and ii) above. Thus, i), the dynamics of neurotransmitter release from presynaptic vesicles should typically affect postsynaptic receptors only minimally and ii), the requirement for 50% receptor activation should be stated in terms of the amount of neurotransmitter reaching the receptor and the rate of agonist-receptor binding. Receptors' response to brief transmitter fluxes therefore follows a different principle from that governing receptor activation in equilibrium, according to which the magnitude of the receptor response is determined by the interplay between the peak transmitter concentration and the receptor affinity for the agonist ($1/K_D$).

Although we could control the amount of neurotransmitter ejected in our experiments, we could not precisely determine the amount of transmitter that reached the receptors because the distance between the receptors and the electrode tip was not constant from experiment to experiment. Thus, we were unable to measure the integral of the concentration timecourse (Q) required to elicit 50% receptor activation experimentally. However, the required Q_{EC50} and Q_{EC90} can be calculated from the receptor kinetic models (Table 1). The amount of transmitter required to evoke 50% or 90% receptor activation is the same for release pulses of either 0.5 or 1 ms duration for four out of six receptors studied. The slight exceptions are AMPAR and AChR, which have fast dissociation kinetics

and smaller values of τ_{int}, and therefore require larger neurotransmitter quanta for EC_{50} activation during release durations as short as 1 ms.

THE EFFECTS OF FUSION PORE OPENING DYNAMICS ON RECEPTOR ACTIVATION

In the light of the above experiments, let us answer the original question – under what conditions can the dynamics of neurotransmitter release through the fusion pore alter the efficacy of quantal synaptic transmission? According to principles ii) and iii), we find that the fusion pore can modify the activation of postsynaptic receptors either via modulating the amount of neurotransmitter released from the vesicles, or by changing the release timecourse, which might affect activation of receptors with the fastest dynamics.

The amount of neurotransmitter that can be released from the vesicles through the fusion pore depends on the product of two factors: the fusion pore conductance and the fusion pore open time. The larger the fusion pore conductance, the shorter the time required for complete neurotransmitter discharge. In the dense-core vesicles of mast cells and large neuronal terminals with the reported fusion pore conductance of 230pS (Breckenridge and Almers 1987; Klyachko and Jackson 2002), neurotransmitter has been estimated to escape from the vesicles completely within a millisecond. Yet, typical fusion pore open times reported in the literature are in the order of hundreds of milliseconds (400-860 ms in (Gandhi and Stevens 2003)). It is therefore unlikely that variations in the fusion pore open time might significantly affect the amount of neurotransmitter released from these vesicles. However, in the microvesicles of the posterior pituitary gland, with fusion pore conductance as low as 19 pS, complete discharge of neurotransmitter might require as long as 5 ms (Klyachko and Jackson 2002). With such low conductance, fusion pore open times shorter than 5 ms might then prevent full neurotransmitter release, and thereby reduce receptor activation. It remains to be seen whether fusion pore open times shorter than 5 ms are physiologically plausible.

The other possibility for how the fusion pore might alter the activation of postsynaptic receptors is by slowing down the rate of fusion pore opening, and thereby prolonging neurotransmitter release. According to principle iii), prolonging neurotransmitter release will more severely attenuate receptors with fast dissociation dynamics rather than receptors with slow dissociation dynamics. Thus, release of neurotransmitter through the narrow fusion pore of 19 pS, which may last up to 5 ms, would only partially activate the fast AMPA receptors (τ_{int} ~ 3ms), but fully activate the slower NMDA receptors (τ_{int} ~ 64 ms). The conductance of the fusion pore is therefore a viable candidate for regulating the strength of quantal synaptic transmission during synaptic plasticity or development. Physiological regulation of the fusion pore has been demonstrated in non-neuronal mammalian cells (Scepek, Coorssen et al. 1998; Fisher, Pevsner et al. 2001; Barclay, Craig et al. 2003), but the possibility of such regulation at small brain synapses yet remains to be established.

APPLICATION TO AMPAR- AND NMDAR– MEDIATED SYNAPTIC TRANSMISSION

Principles i) and ii) can be further applied to explain the "paradoxical" behavior of ligand-gated receptors during synaptic transmission. In particular, the peak concentration of glutamate during synaptic transmission can reach 2-3 mM (Clements 1996), which is an order of magnitude higher than the equilibrium K_D of AMPA receptors (K_D ~ 400 μM) and three orders of magnitude higher than the equilibrium K_D of NMDA receptors (K_D ~ 2.6 μM)(Patneau and Mayer 1990). This high concentration of glutamate would therefore saturate both receptors in equilibrium conditions. Yet, during synaptic transmission, neither receptor is saturated by this high glutamate concentration (Bekkers, Richerson et al. 1990; Liu and Tsien 1995; Forti, Bossi et al. 1997; Liu, Choi et al. 1999; Mainen, Malinow et al. 1999; McAllister and Stevens 2000; Ishikawa, Sahara et al. 2002; Oertner, Sabatini et al. 2002). This can be explained by principle i), according to which, during fast synaptic transmission, receptor activation is determined by the integral of the concentration time

course of neurotransmitter in the synaptic cleft, not merely by its peak. Thus, glutamate fails to saturate both receptor types because it remains at such high concentration only briefly (~100 μs) (Clements 1996). The time integral of the concentration (2mM*100 μs) is then not sufficient to saturate the receptors, given their relatively slow rate of glutamate binding (AMPA k_1 ~ 0.005; NMDA k_1 ~ 0.005). Interestingly, according to principle ii), the same neurotransmitter time course might fully saturate receptors with faster binding kinetics, such as acetylcholine receptors (k_1 ~ 0.1). This correlates with physiological observations (Matthews-Bellinger and Salpeter 1978; Dionne 1981). Second, AMPA and NMDA receptor currents during synaptic transmission are highly correlated (McAllister and Stevens 2000), despite the fact that their affinities to glutamate vary by 100-fold. This can be explained by principle ii), according to which the degree of receptor activation during synaptic transmission is largely determined by the binding rate of the ligand with the receptor. The fact that AMPA and NMDA receptor currents during synaptic transmission are highly correlated is therefore a consequence of their similar binding rates of glutamate (AMPA k_1 ~ 0.005 $\mu M^{-1}ms^{-1}$; NMDA k_1 ~ 0.005 $\mu M^{-1}ms^{-1}$)(Jonas and Sakmann 1992; Chen, Ren et al. 2001).

GENERAL EFFECTS OF THE TIMECOURSE OF NEUROTRANSMITTER IN THE SYNAPTIC CLEFT ON RECEPTOR ACTIVATION

Finally, based on equation (1), we can interpret the effects of general neurotransmitter timecourse in the synaptic cleft on the magnitude of the postsynaptic response. According to equation (1), receptor activation during brief transmitter fluxes is proportional to the integral of the agonist concentration timecourse. Therefore, any factor that will enhance the timecourse of neurotransmitter, either by increasing its peak or duration, should potentially increase the magnitude of receptor currents. One factor that affects the slow component of the neurotransmitter timecourse in the synaptic cleft, without significantly affecting the peak concentration, is the rate of neurotransmitter reuptake and enzymatic degradation. Blocking either mechanism should therefore enhance receptor

activation by prolonging neurotransmitter timecourse; this has been shown in multiple preparations, although the results have not been uniformly consistent (Isaacson and Nicoll 1993; Tong and Jahr 1994; Kidd and Isaac 2000). Extrasynaptic diffusion barriers should also slow down the clearance rate of glutamate from the synapse without significantly affecting the peak concentration (Clements 1996). Accordingly, slowing down extrasynaptic diffusion of glutamate by dextran has been shown to augment receptor activation (Min, Rusakov et al. 1998). Conversely, addition of an enzymatic glutamate scavenger, which speeds up the rate of glutamate clearance, should reduce the postsynaptic response, consistent with observation (Min, Rusakov et al. 1998).

However, the effect of a prolonged neurotransmitter timecourse on the degree of receptor activation will depend on the receptors' integration time constant τ_{int}. A prediction of our model is that the NMDA receptor currents should be enhanced more by the above perturbations than the currents of AMPA receptors, which are worse than NMDA receptors in responding to prolonged neurotransmitter flux. An extreme instance of this effect can be observed during glutamate spillover between adjacent synapses, which generates an extremely long (~100 ms) and low concentration of agonist in the synaptic cleft. Accordingly, NMDA receptors have been shown to be much more likely activated by glutamate spillover than AMPA receptors (Kullmann, Erdemli et al. 1996; Asztely, Erdemli et al. 1997).

Another important factor that will affect the concentration timecourse of transmitter at the receptor is the diffusional distance between the receptor and the release site. Both the lateral displacement of the receptor from the release site and the width of the synaptic cleft should therefore play a crucial role in modulating the degree of endogenous receptor activity. Our simulations indicate that radial displacement of 0.2 μm might reduce receptor activation by twofold. This can be compared to the sensitivity of the receptors to the lateral displacement from the release site in detailed Monte Carlo simulations, which report an even shorter spatial sensitivity constant of 0.1 μm (Franks, Stevens et al. 2003).

METHODS

Patch Clamp Electrophysiology

Primary cultures of CA1-enriched hippocampal neurons were prepared from neonatal rats (P1) as described previously (Liu, Choi et al. 1999). The age of the cultures ranged from 8 to 16 days *in vitro* (DIV). The composition of the extracellular solution in patch clamp recordings was (in mM): NaCl 145, KCl 3, $CaCl_2$ 2.6, $MgCl_2$ 1.3, glucose 10, glycine 0.005, HEPES 10 (adjusted to pH 7.4 with NaOH), and tetrodotoxin (TTX, 0.5 μM). $MgCl_2$ was absent in the recordings of synaptic NMDAR currents. In both AMPAR and NMDAR synaptic recordings, the intracellular solution contained (in mM): K-gluconate 120, KCl 7, HEPES 10, NaCl 8, $CaCl_2$ 0.5, EGTA 5, MgATP 2, NaGTP 0.3, adjusted to pH 7.25 with KOH. In $GABA_AR$ recordings, the intracellular solution contained (in mM): CsCl 125, $TEACl_4$ 10, HEPES 10, NaCl 8, $CaCl_2$ 0.06, EGTA 0.6, MgATP 4, NaGTP 0.3, adjusted to pH 7.2 with CsOH. For all outside-out patch recordings the intracellular solution contained (in mM): $CsMeSO_3$ 120, HEPES 10, NaCl 8, $CaCl_2$ 1, EGTA 10, MgATP 2, NaGTP 0.3, adjusted to pH 7.25 with CsOH. Synaptic and outside-out AMPAR currents were recorded at –60 mV in the presence of 1.3 mM extracellular Mg^{2+}, which minimized the NMDAR current component. Synaptic NMDAR currents were recorded at –60 mV, in 0 mM extracellular Mg^{2+}, in the presence of 5μM NBQX, which blocked the AMPAR current. Outside-out NMDAR currents were recorded at +40 mV, in 1.3 mM Mg^{2+} and 0.5 mM Ca^{2+}, in the presence of 10 μM SYM 2206 (Tocris) to block the AMPAR current. Dual recordings of AMPA and NMDA currents (Fig. 5) were obtained from the same excised patch, in 1.3 mM extracellular Mg^{2+}; the AMPA current was recorded at –60 mV, the combined current was recorded at +40 mV. Synaptic GABA currents were recorded at –60 mV; the reversal potential of Cl^- in these experiments was set to 0 mV by adding 125 mM CsCl into the patch solution. GABA currents thus appear as inward current events. GABA

currents in excised patches were recorded at 0 mV with regular Cl^- concentration; the currents appeared as regular outward events. All currents were filtered at 1 kHz and sampled at 20 kHz.

Iontophoresis System

The details of the iontophoresis technique can be found in our previous publication (Murnick, Dube et al. 2002). Briefly, iontophoresis microelectrodes were fabricated from quartz glass capillary tubes (O.D. = 1.0 mm, I.D. = 0.7 mm) and pulled in a single stage with a horizontal pipette puller P-2000 (Sutter Instruments Co., Novato, CA), achieving tip diameter of ~0.1 μm and a resistance of 150-200 MΩ when filled with 150 mM glutamatic acid (pH adjusted to 7.0 with NaOH), and 500 mM GABA (pH adjusted to 3.0) respectively. Negative currents were applied to drive ejection of glutamate with a net negative charge at neutral pH. Positive currents were applied to eject GABA which has a net positive charge at pH 3.0. Current ejection was performed with the MVCS 02 (NPI Electronic, Tamm, Germany) current clamp system. The time-constant of the stimulating electrode was electronically compensated until the voltage pulse generated by a square current injection appeared perfectly rectangular. Although a background holding current is typically used to prevent neurotransmitter leakage, we omitted the holding current in order to ensure linear response of the electrode. In most of experiments, because of the small diameter of the electrode tip, neurotransmitter did not leak significantly from newly fabricated electrodes. The absence of neurotransmitter leak was verified by the effects on receptor desensitization: if 0.5 nA iontophoretic holding current caused a significant (>10%) increase in the magnitude of the evoked receptor currents, the residual leak was assessed as significant and the electrode was replaced. The residual leak of the electrode often increased after touching the lipid cell membrane.

Properties of neurotransmitter delivery through the iontophoresis electrode

The properties of the iontophoresis device were monitored by ejection of Oregon Green fluorescent dye. Dye fluorescence was measured with the confocal microscope point scan

function at ~0.5 μm distance from the electrode tip along the main electrode axis. The timecourse of the fluorescence was fit with the solution to the diffusion equation from a point source with an injection rate *r* for the duration *T*

$$C(d,t) = r \int_{\max(t-T,0)}^{t} (4\pi D t')^{-N/2} \exp\left(-d^2/4Dt'\right) dt' \qquad (2)$$

where D is the diffusion constant (0.53 $\mu m^2/ms$ for Oregon Green), *d* is the distance from the electrode tip (data fit = 0.69 μm), and N is the dimensionality of diffusion. As transmitter diffused in a free medium, the dimensionality of diffusion was set to N=3 in the fits in Fig. 1B. However, we obtained better fits to the fluorescence timecourse in Fig. 1C with N=2 (RMSE = 10.68) rather than N=3 (RMSE = 19.86). The discrepancy was likely caused by the fact that the confocal microscope integrated fluorescence across a thin ~1 μm z-section of the specimen. As the bulk of the released dye within the first 2 ms after the release would stay within the 1 μm slab integrated by the confocal optics (mean diffusional distance in 2 ms being $\sqrt{2ms \cdot 0.53\mu m^2 ms^{-1}} = 1.03\mu m$), this would have contributed to the apparent reduction of the dimensionality of diffusion to two dimensions during the first 2 ms from the release onset. This short 2 ms interval contributed most to the fitting error with N=3; the remaining timecourse was well fit with N=3.

The integrated fluorescence (proportional to the amount of released fluorescent dye) was linear in the duration and magnitude of the applied current for currents in the range 2nA – 200 nA. Below 2 nA, the device behaved slightly sub-linearly. On the other hand, currents greater than ~200 nA (depending on the resistance of the electrode) saturated the current clamp system. Thus, recordings evoked by > 200 nA currents have been omitted in most figures, whereas recordings with <2 nA currents underestimate the receptor response.

Activation of synaptic receptors

Individual synapses were visualized with the FM1-43 fluorescent dye (Molecular Probes, Eugene, OR). The composition of the staining solution was (in mM): NaCl 105, KCl 40, HEPES 10, glucose 10, $CaCl_2$ 2.6, $MgCl_2$ 1.3, kyneurinic acid 0.5, and FM 1-43 0.01 (adjusted to pH 7.4 with NaOH). Following a one-minute incubation time in the staining solution and a >5 min wash, neurons were visualized under a confocal microscope using a 40x planachromat water immersion objective (1.15 NA). To ensure activation of single synapses, we selected cells in early stages of development (DIV 12 and earlier), and regions with low synaptic densities (<1 synapse / 8 μm), as determined by FM1-43 functional synaptic staining. The pipette with the neurotransmitter was positioned as close as possible to the synapse (~ 0.5 μm) without incurring damage to the synaptic structure. Activation of single synaptic sites was verified by the fact that no detectable response was recorded if the pipette was moved 3μm away from the synaptic site – a distance smaller than half the synaptic separation.

Data fits.

All data points (29 or 30) displayed in Figs. 3-6 were least-squares fitted by equation (1) in a single session as follows: The values of k_1 (the agonist binding rate) and N were constrained (see below). For each data point, the value for T (the length of the ejection pulse) was constrained. Q was calculated from the total delivered iontophoretic charge (Φ) as $Q=\Phi/R$, where R was left as a free parameter corresponding to the variable distance between the electrode tip and receptor patch. All data points were therefore fitted with 3 free parameters: R, I_{max}, and τ_{inf}. I_{max}, the maximum obtainable current through the patch, depended on the single channel current at full saturation and the number of receptors located in the membrane patch or synapse, which varied between experiments; it is therefore not reported. N, corresponding to the number of occupied binding sites required for receptor activation, was constrained at 2 for AMPA, NMDA, acetylcholine, and kainate receptors, 1 for serotonin receptors (since the second binding step is 10x slower than the

first binding step (Zhou, Verdoorn et al. 1998), receptor activation is dominated by a single binding step) and 2 for $GABA_A$ receptors (since the fraction of open receptors in a single occupied state is 100x smaller than the fraction of open receptors in the double bound state; the contribution to the total current from receptors binding a single neurotransmitter is therefore negligible).

APPENDIX

To analyze the effects of the application timecourse of a fixed neurotransmitter amount (Φ) on the degree of receptor activation, we first analyze the effects of the application timecourse on receptor occupancy, and then consider the effects on receptor current.

Single binding site occupancy

Suppose that ejection of a fixed neurotransmitter amount Φ generates the concentration timecourse A(t) (A for agonist) at the receptor. The reaction kinetics for a single receptor binding site follows the scheme:

$$R \underset{k_2}{\overset{k_1 A(t)}{\rightleftharpoons}} AR,$$

where k_1 is the rate of agonist binding, k_2 the rate of agonist dissociation, and A(t) is the agonist concentration timecourse. The general solution for fractional receptor occupancy based on this kinetic scheme is

$$AR(T) = 1 - e^{-k_1 \int_0^T A(t)dt - k_2 T} \left(1 + k_2 \int_0^T e^{k_1 \int_0^t A(t')dt' + k_2 t} dt \right) \tag{3}$$

If the ejection pulse is much shorter than the time constant of dissociation ($Tk_2 << 1$), the effects of dissociation can be neglected, and the peak receptor occupancy (occurring at the end of the concentration transient) will be given by

$$AR_{peak} = 1 - e^{-k_1 Q}, \tag{4}$$

where $Q = \int_0^\infty A(t)\,dt$. The quantity $Q = \int_0^\infty A(t)\,dt$ is independent of the temporal profile of neurotransmitter ejection (this is a characteristic of point source diffusion) and is proportional to $\Phi/4\pi DR$, where Φ is the amount of ejected neurotransmitter, R is the

distance between the ejection site and the receptor, and D is the diffusion constant. (We neglect the effects of scavenger molecules and enzymatic degradation on the timecourse A(t), which might affect Q in the case of different ejection profiles in a real synapse). Therefore, during short ejections ($T << 1/k_2$), receptor occupancy will depend on the amount of released neurotransmitter Φ, but will be independent of the particular dynamics of its ejection. The receptor therefore behaves as a perfect molecular integrator of the agonist.

However, as the neurotransmitter ejection pulse prolongs, dissociation can no longer be neglected. The general solution to receptor occupancy in this case is given in equation (3) . However, this formulation does not offer much insight into receptor's behavior as an integrator – in particular, the effects of the duration of ejection of a fixed neurotransmitter amount on receptor response are not clear. For better tractability, we therefore analyze the situation in which the concentration timecourse at the receptor approximates a rectangular shape of magnitude A and duration T. Although this is a simplification, it can be used as a first approximation to generate insight into the receptor behavior. In this case, the peak receptor occupancy (incident with the end of the concentration pulse) is given by

$$AR_{peak} = AR_{\infty}\left(1 - e^{-\lambda T}\right) \tag{5}$$

$$AR_{\infty} = \frac{A}{A + k_2/k_1} = \frac{A}{A + K_D} \qquad \lambda = Ak_1 + k_2$$

where $K_D = k_2/k_1$ is the receptor-ligand dissociation constant, AR_{∞} is receptor occupancy in the limit ($T \rightarrow \infty$), and λ is the eigenvalue of the reaction scheme. Equation (5) can now be rewritten in a form that states the behavior of the receptor as that of a leaky integrator – the peak occupancy is a product of an ideal integrator of the ejected neurotransmitter (equivalent to (4)), which is invariant under the timecourse of ejection, and the "leak" term, which quantifies the effects of the period over which neurotransmitter Φ is ejected on the size of the response:

$$AR_{peak} = \underbrace{\left(1-e^{-k_1 Q}\right)}_{Integrator}\underbrace{e^{-T/\tau}}_{Leak} \quad \tau = \left(1+0.32k_1 Q\right)\tau_{\text{int}} \qquad (6)$$

Here, Q=AT, and $\tau_{int}=2.2/k_2$. Equation (6) approximates equation (5) within 3% (absolute) error as long as $k_1Q < 3$ and $k_2T < 3$; that is, up to 95% receptor saturation and up to three time constants into the reaction time of the system, which accounts for 95% of the receptor's dynamics before reaching equilibrium. Based on this formulation, we can define the receptor ***integration time constant*** τ_{int} as the length of the release pulse that will cause an e-fold reduction in the receptor occupancy evoked by a small neurotransmitter amount ($\Phi,Q\rightarrow 0$) as compared to the occupancy evoked by an instantaneous release of the same neurotransmitter amount. The integration time constant is therefore a measure of how well the receptors respond to slower and more prolonged fluxes of a fixed transmitter amount Φ; it is an intrinsic property of the receptor and can be measured experimentally. In the above reaction scheme, $\tau_{int}=2.2/k_2$ is inversely proportional to the dissociation rate k_2 and therefore proportional to the deactivation time constant of the receptor.

Receptors with gating

The simplest receptor activation scheme including receptor gating is the following:

$$R \underset{k_2}{\overset{k_1 A(t)}{\rightleftharpoons}} AR \underset{\alpha}{\overset{\beta}{\rightleftharpoons}} AR^*$$

For most ligand-gated receptors, receptor gating is significantly faster than dissociation (i.e., $\alpha+\beta >> k_2$). In such case, the opened and closed kinetic states equilibrate fast, and the kinetic states AR and AR^* can be collapsed into a single state AR/AR^*. The fraction of receptors in the open state is then proportional to the overall receptor occupancy, scaled by the factor $\frac{\beta}{\alpha+\beta}$. The dynamics of this reaction therefore effectively becomes:

$$R \underset{k_2\alpha/(\alpha+\beta)}{\overset{k_1 A(t)}{\rightleftharpoons}} AR/AR^*$$

which is similar to the previous case. This yields the solution

$$AR^{*}_{peak} = \frac{\beta}{\alpha+\beta}\left(1-e^{-k_1 Q}\right)e^{-T/\tau} \qquad \tau = \left(1+0.32k_1 Q\right)\tau_{int}$$

where the integration time constant $\tau_{int}=2.2/(k_2\alpha/(\alpha+\beta))$ again is a constant multiple of the receptor deactivation time constant $\tau_{deac}=(\alpha+\beta)/k_2\alpha$.

Receptors with multiple binding sites

If receptor opening requires simultaneous binding of N receptor subunits, receptor current will be proportional to the probability of simultaneous occupancy of all N binding sites, which equals the probability of single binding site occupancy (equation (6)) raised to the power of N (if binding of different receptor subunits is independent). Thus,

$$A_n R_{peak} = \left(1-e^{-k_1 Q}\right)^N e^{-T/\tau} \qquad \tau = \left(1+0.32k_1 Q\right)\tau_{int}$$

where $\tau_{int}=2.2/(k_2 N)$. Thus, the greater the number of binding sites required for receptor activation, the shorter the receptor's τ_{int}, and the worse the receptor's ability to integrate slow neurotransmitter delivery.

In the case of allosteric interaction between different receptor subunits or subunits with different agonist affinities, if the discrepancy between the rates of binding of different subunits is large, receptor kinetics will be dominated by the slowest binding kinetic step, or the binding site with the lowest affinity for the agonist. The effective number of receptor subunits that control receptor gating is then reduced. Thus, for instance, the peak currents of serotonin receptors during brief neurotransmitter applications are best described by N=1, since the second binding kinetic step is 10x slower than the binding of the first neurotransmitter; the kinetic reaction is therefore dominated by a binding step (Zhou, Verdoorn et al. 1998).

Receptors with Gating and Desensitization

To examine the effects of desensitization on the peak receptor current, we considered the simplest receptor activation scheme, in which gating is significantly faster

than desensitization and therefore can be collapsed to a single state (this assumption holds true for most receptors):

$$R \underset{k_2}{\overset{k_1 A(t)}{\rightleftharpoons}} AR/AR^* \underset{\gamma}{\overset{\delta}{\rightleftharpoons}} AR_d$$

To examine the effects of the desensitization rate constant δ on the integrative properties of this receptor scheme, we simulated the response of this scheme to a number of square pulse protocols, such as in Fig. 6. We fixed $k_2 = 0.5$ ms^{-1} and $\gamma = 0.1$ ms^{-1}, consistent with the fact that recovery from desensitization occurs much slower than dissociation in most receptors, and varied the rate into desensitization δ between 0.1 and 0.9 ms^{-1}. Thus, δ was tested in the range from where desensitization is much slower than dissociation (e.g. NMDA receptors) to where desensitization is comparable to or faster than dissociation (e.g. AMPA receptors). Under all conditions, the magnitude of the receptor response was well described by equation (6). Furthermore, the values of τ_{int} obtained from the data by fits with equation (6) were tightly correlated with the values of τ_{deact} under all conditions ($R^2 = 0.99$). Thus, τ_{int} is related to both the rate of dissociation and desensitization, and is proportional to τ_{deact}.

FIGURE LEGENDS

Figure 1. Kinetic release properties of the iontophoresis device

(A) Neurotransmitter containing electrode positioned over a single synaptic site on the hippocampal dendrite. (B) Fluorescence of the Oregon Green dye in the units of the PMT counter, measured at ~0.5 μm from the tip of the electrode along the main axis after applying 8 nA currents over 0.25-8 ms. The integral of the fluorescence signal is a linear function of the pulse duration (inset). Smooth lines are fits with the solution to the point source diffusion equation (equation **(2)**; see Methods). (C) Dye fluorescence generated by 1 ms ejection currents of 25-200 nA magnitude. The fluorescence peak is a linear function of the current amplitude (inset). (D) Estimated glutamate concentration timecourse generated by free diffusion from the electrode tip (N=3, D = 0.75 $\mu m^2/ms$) at d = 0.5 μm distance. Estimates are based on release pulses of T=0.5,1,2,4,8 and 16 ms duration, and current magnitudes $I=\Phi/T$ which eject a constant amount of neurotransmitter. Concentration units are normalized as they depend on the amount of released transmitter and the charge-to-released-glutamate yield of the iontophoresis device. (Inset) Simulated glutamate concentration timecourse generated by diffusion of glutamate in a cylindrical synaptic cleft (N=2, D = 0.2 $\mu m^2/ms$) at d = 0.04 μm radial distance from the vesicle release site. Diffusion coefficient in the synapse is approximately a third of that in the aqueous environment due to molecular overcrowding (Franks, Bartol et al. 2002). Timecourse is based on fusion pore open times of T=0.5,1,2,4,8 and 16 ms duration, and fusion pore conductances that preserve the total amount of released neurotransmitter.

Figure 2. Timecourse of neurotransmitter delivery has different effects on the activation of AMPA, NMDA, and $GABA_A$ receptors.

Iontophoretic pulses of duration 0.5, 1, 2, 4, 8 and 16 ms and current magnitudes of 128, 64, 32, 16, 8, and 4 nA were applied. The conserved electric charge delivered (64 pC)

was low enough to evoke about 70% maximum response, and avoid receptor saturation. (Top) Estimated transmitter concentration timecourse at 0.5 μm distance from the electrode tip, based on the numerical solution to the point-source diffusion equation **(2)**. Concentrations are in arbitrary units, as the absolute magnitude of the concentration depended on the charge-to-released-glutamate yield of the iontophoretic device, as well as the distance between the electrode tip and the receptors, which was undetermined. At distances closer than 0.5 μm, the concentration waveforms would appear more sharp and rectangular. (Bottom) Evoked currents recorded from AMPA, NMDA, and $GABA_A$ receptors in excised patches. The currents are averaged over 5 recordings from a single patch for each receptor type.

Figure 3. The effects of the ejection timecourse of glutamate on the activation of NMDA receptors

(A) Average (n=5) NMDA receptor currents evoked by iontophoresis pulses of duration and magnitude as indicated. Current magnitudes increased as powers of 2. Traces of equal color correspond to ejection pulses that preserve the amount of released neurotransmitter. (B) Peak receptor currents as a function of the ejection duration and neurotransmitter amount (Φ). Φ is reported in units of iontophoretic charge. Solid lines are fits by equation (1) (χ^2 = 12.08; d.o.f. 26; $p > 0.99$). Horizontal fit lines indicate that the receptor currents were independent of the dynamics of neurotransmitter ejection. τ_{int} is reported with 95% accuracy. (C) Peak receptor currents as a function of the estimated peak neurotransmitter concentration (based on estimates in Fig. 1D). Concentrations are stated in arbitrary units as they depend on the distance between the electrode tip and the receptors, and the iontophoretic-charge-to-glutamate yield of the iontophoresis electrode. Error bars are standard deviations of the current peaks obtained from five recordings on a single patch; spread resulted from a combination of the stochastic nature of channel opening and drift in the electrode position during experiments. (D) Peak receptor currents as a function of the amount of released glutamate. Fit by the Hill equation (χ^2/d.o.f. = 0.15; $p > 0.99$) yielded a Hill coefficient N=1.93±0.09.

Figure 4. The effects of neurotransmitter ejection timecourse on the activation of AMPA and $GABA_A$ receptors

(Top) Average AMPA and $GABA_A$ receptor currents (n=5) recorded from a single outside-out patch, in response to iontophoresis release as in Fig. 3. (Bottom) Peak receptor currents analyzed as a function of the duration of neurotransmitter release pulse. Error bars are standard deviations of the measured current peaks. Solid lines are fits with equation (1) (AMPAR currents: $\chi^2 = 17.24$; d.o.f. 26; $p = 0.90$; $GABA_AR$ currents: $\chi^2 = 14.17$; d.o.f. 26; $p = 0.97$).

Figure 5. Activation of synaptic AMPA, NMDA and $GABA_A$ receptors by different temporal delivery profiles of neurotransmitter

(Top) Average currents recorded from AMPA (n=4), NMDA (n=2) and GABA (n=3) receptors located at isolated synapses of cultured hippocampal dendrites. (Bottom) Peak receptor currents as a function of the neurotransmitter pulse duration; solid lines are fits with equation (1). (AMPA receptors: $\chi^2 = 13.0$, $p = 0.98$; $GABA_A$ receptors: $\chi^2 = 23.61$, $p = 0.6$; NMDA receptors: $\chi^2 = 12.33$, $p = 0.99$; d.o.f. = 26).

Figure 6. Response of receptor kinetic models to different temporal delivery profiles of neurotransmitter

Simulated peak receptor probability of opening (P_o) evoked by rectangular release pulses of different durations and magnitudes, such as those in Figs.3-5. Simulations were based on the following receptor kinetic models: AMPA (Jonas, Major et al. 1993), NMDA (NR2A) (Chen, Ren et al. 2001), $GABA_A$ (Jones and Westbrook 1995), acetylcholine (AChR) (Colquhoun and Sakmann 1985), kainate (GluR6) (Heckmann, Bufler et al. 1996), and serotonin (5HT-3) (Zhou, Verdoorn et al. 1998).

Figure 7. Receptor integration time constant (τ_{int}) is correlated with the deactivation time constant (τ_{deact})

(A) Responses to different glutamate timecourse from slow AMPA receptors on a pyramidal neuron, fast AMPA receptors on an interneuron, and the receptors from the same cell with desensitization blocked by 100 μM cyclothiazide. (B) Correlation between τ_{int} and

τ_{deact} obtained in multiple experiments from synaptic AMPA receptors with different kinetic properties. (C) Correlation across multiple receptor species. Each data point corresponds to either an average recording obtained from an outside-out patch (out), a synaptic recording (syn), or a simulation (sim).

Figure 8. AMPAR/NMDAR current ratio as a function of duration of glutamate delivery

(A) Dose response curves of AMPA and NMDA receptors to glutamate pulses of 0.5 ms duration. (B) AMPA and NMDA receptor activation ratio by ejections of different durations. (C) Selective activation on NMDA receptors in synapses containing both AMPA and NMDA receptors – "silent" synaptic transmission.

FIGURES

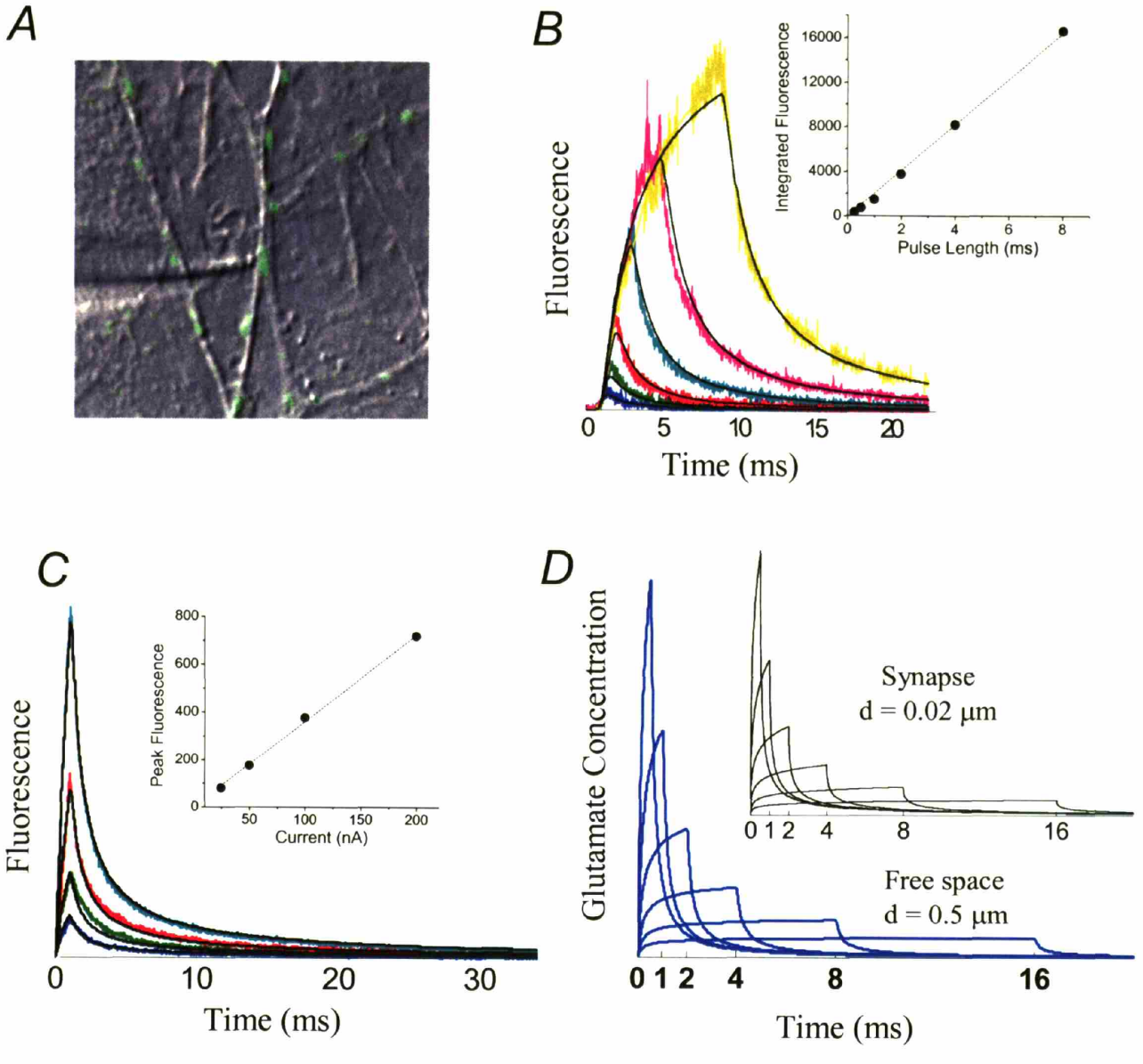

Figure 1

Krupa et al.

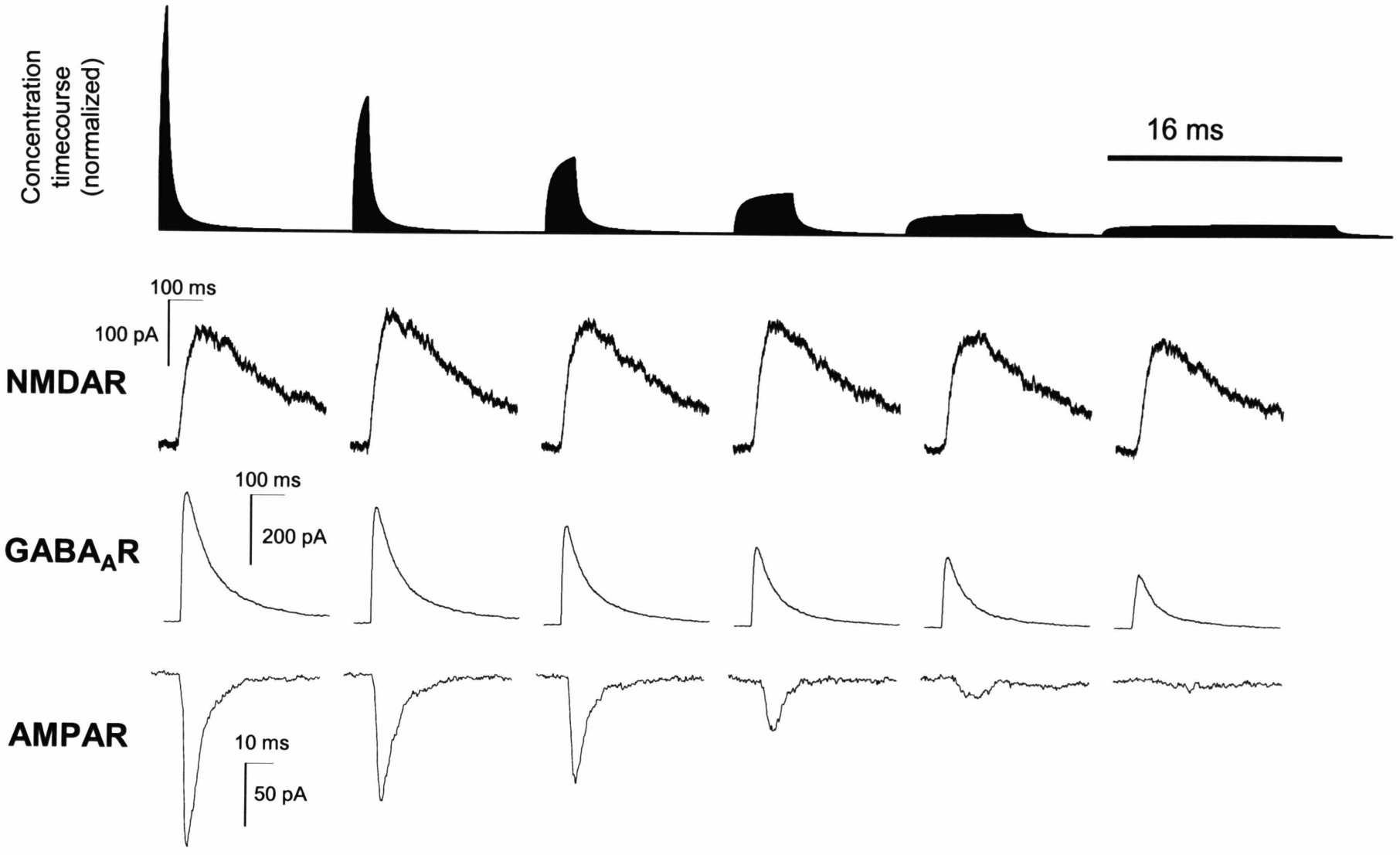

Figure 2

Krupa et al.

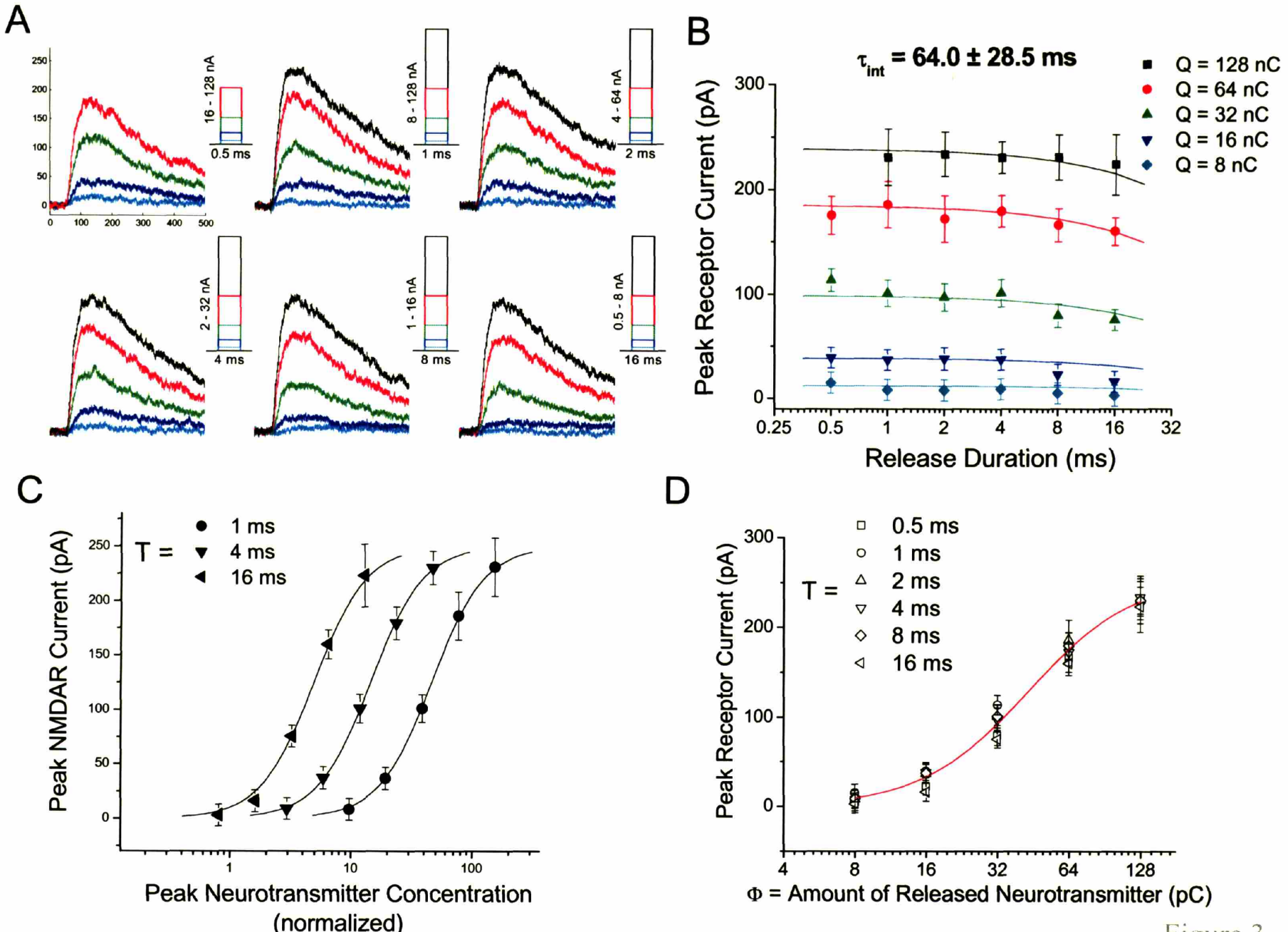

Figure 3
Krupa et al.

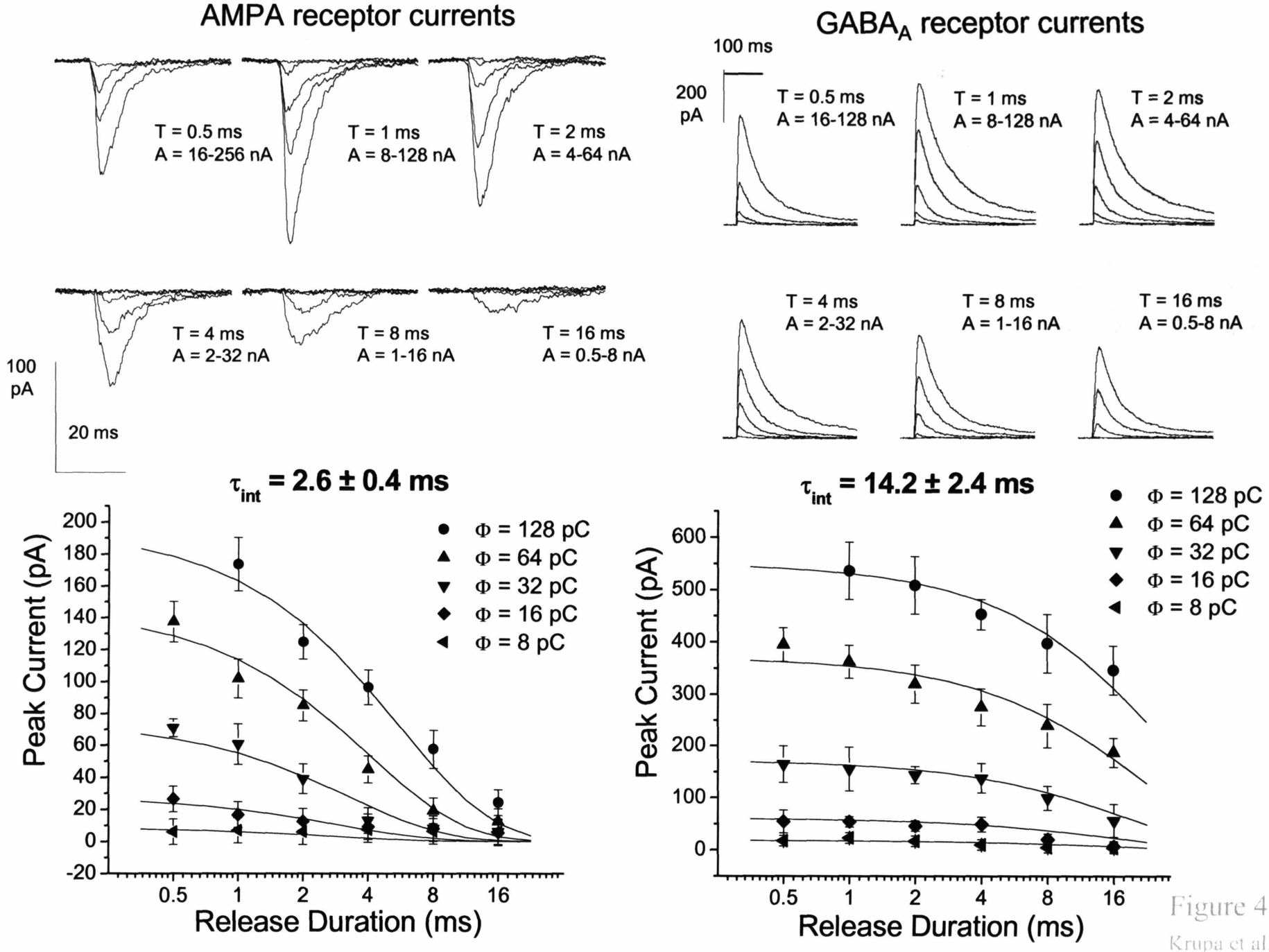

Figure 4

Krupa et al.

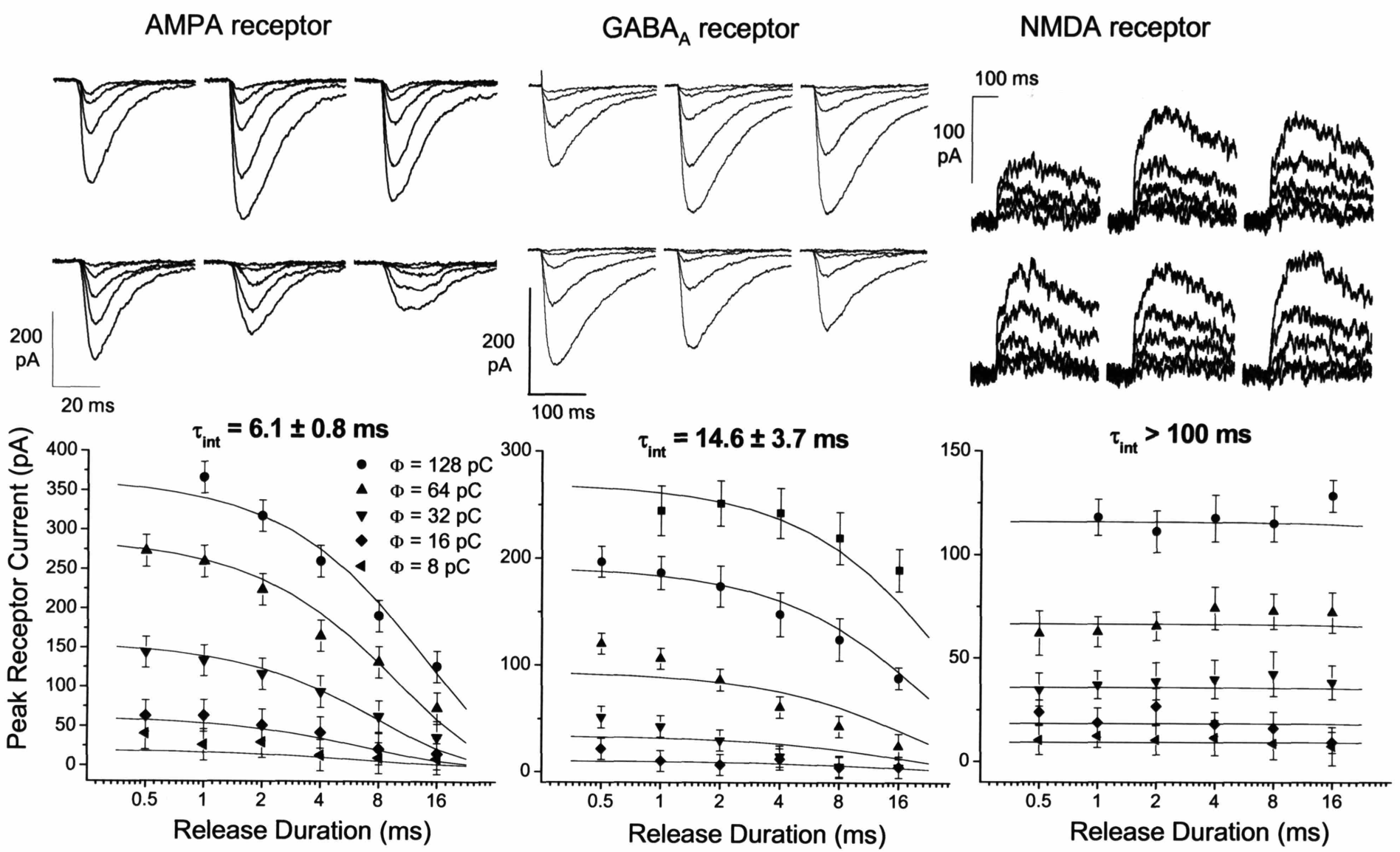

Figure 5

Krupa et al.

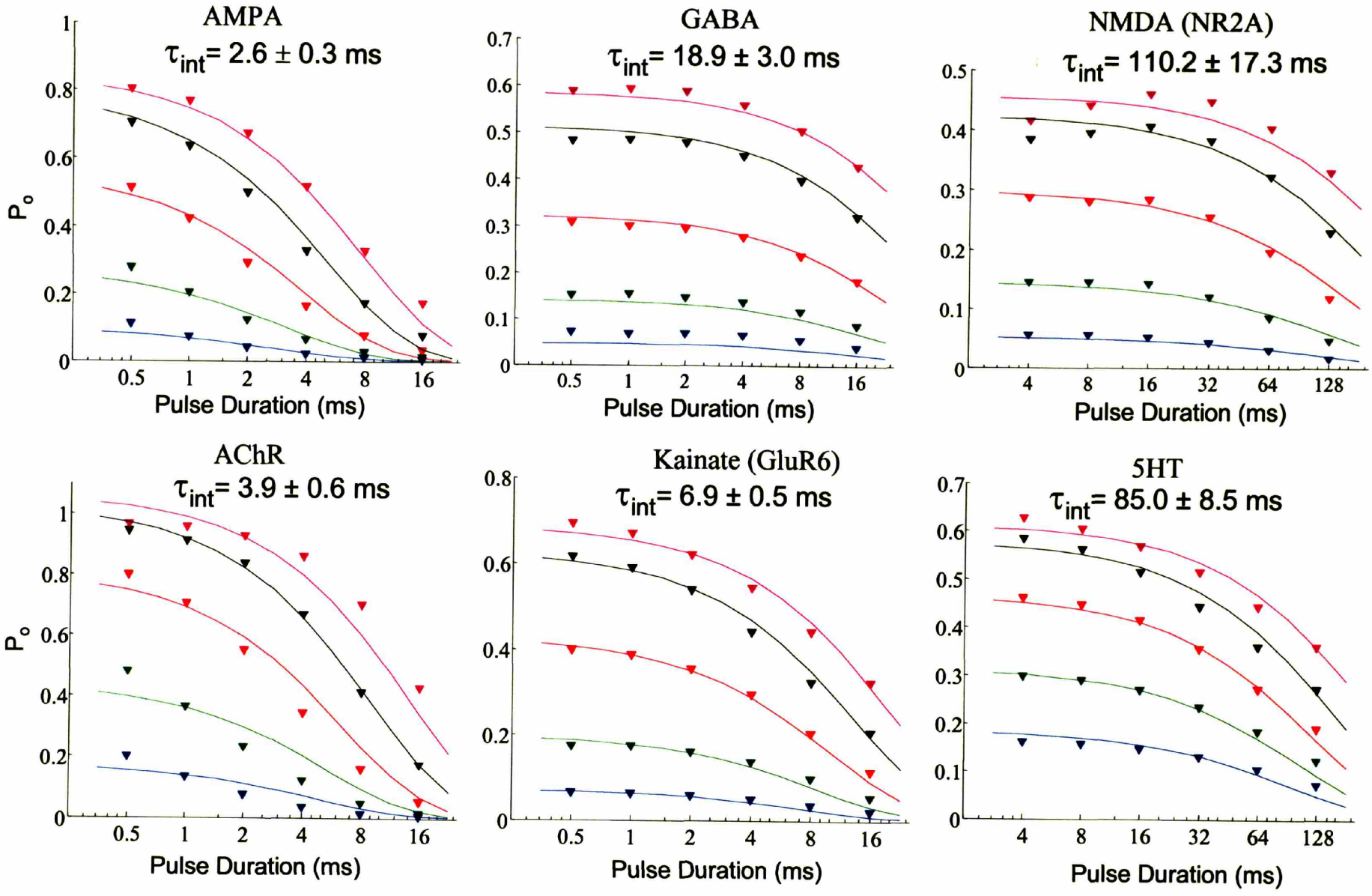

Figure 6
Krupa et al.

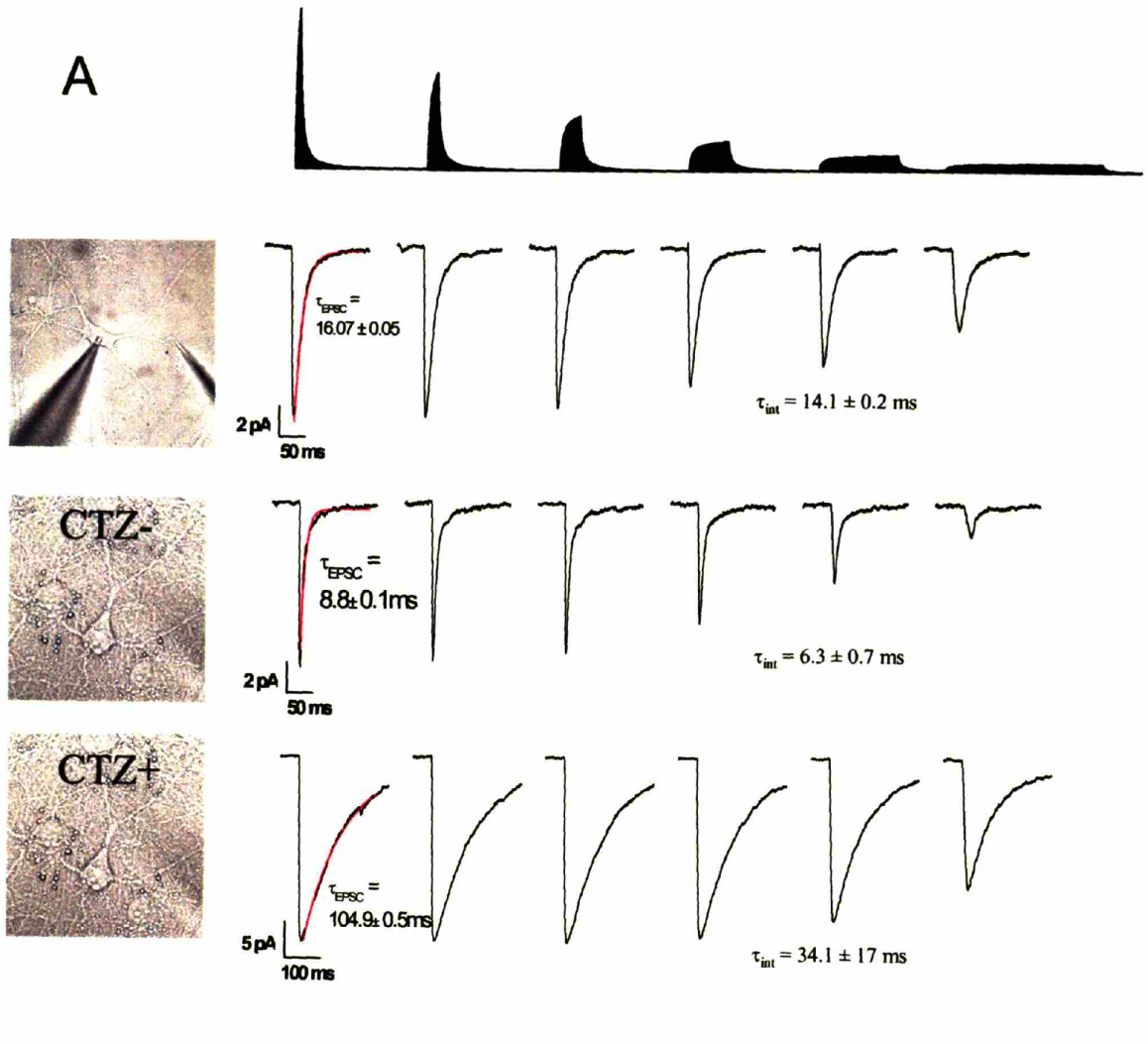

Figure 7

Krupa et al.

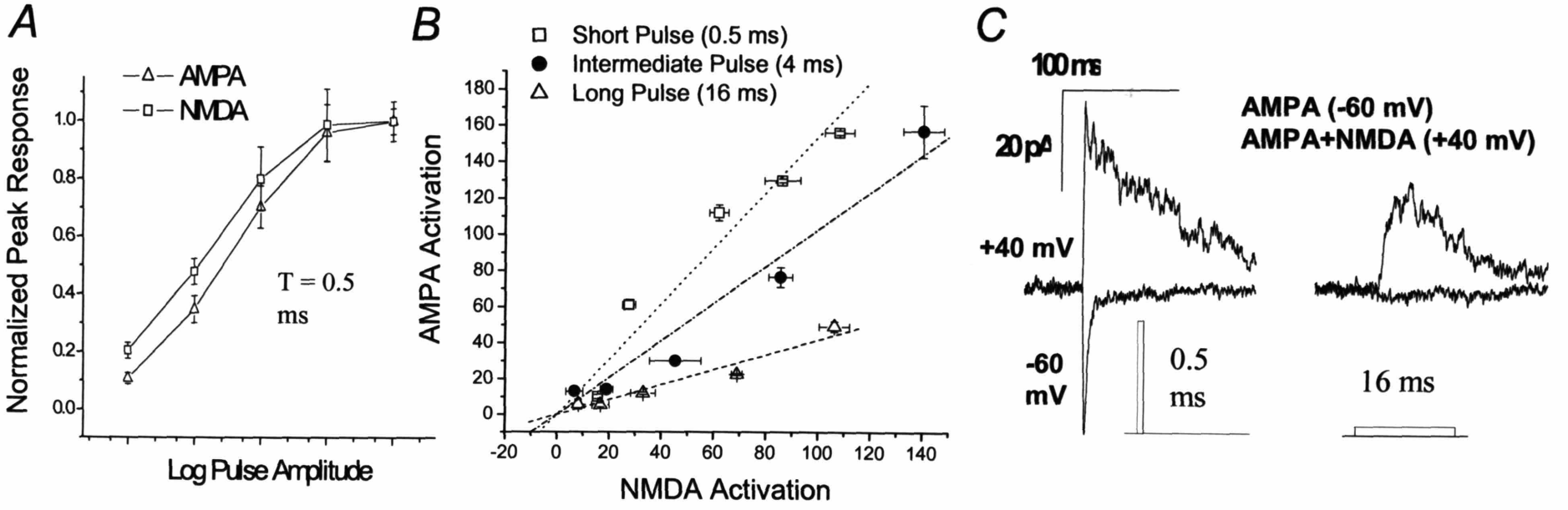

Figure 8
Krupa et al.

Table 1.

% Activation	AMPAR μM·ms	NMDAR μM·ms	$GABA_AR$ μM·ms	AChR μM·ms	GluR6 μM·ms	5HT μM·ms
50 % (.5 ms flux)	324	257	409	25.5	360	853
50 % (1 ms flux)	425	258	414	32.5	366	850
90 % (.5 ms flux)	1210	624	1160	66.8	913	2410
90 % (1 ms flux)	1570	650	1170	82.1	1010	2410

Table 1
Krupa et al.

Table 2. Comparison of Receptor Activation in Equilibrium and During Quantal Release

Equilibrium	Quantal Release
Concentration detector: $I = I_{\max}\left[\frac{A}{A+K_D}\right]^N$ Response depends on: • Affinity K_D • Transmitter concentration A	Molecular Integrator: $\tau = (1+0.32k_1Q)\tau_{\text{int}}$ $I = I_{\max}\left(1-e^{-k_1Q}\right)^N e^{-T/\tau}$ $\quad Q = \int_0^T A(t)\,dt$ Response depends on: • Binding rate k_1 • Amount of transmitter reaching the receptor Q • Ratio of release duration T and integration time constant τ_{int}

III. INHIBITION MEDIATES DENDRITIC SENSITIVITY TO THE DIRECTION OF SYNAPTIC ACTIVATION

SUMMARY

The ability of brain cells to discriminate the order of firing of their synaptic inputs could be potentially important for neuronal encoding, memorization, and decoding of temporal sequences of events by the brain – for instance, the temporal sequence of activation of retinal rods and cones by a light stimulus moving in a certain direction recognized by retinal ganglion cells, the order of activation of hippocampal place cells of a rat moving within a maze, or the order of digits comprising a phone number during a memorization task. Several theories have been put forth to explain how the brain can encode temporal series, however, whether this computation can occur at the level of individual neurons or requires a larger neural network is still unclear. Even if individual neurons were capable of computing this task, how exactly they perform this computation poses further questions. Here, also, several theories exist. One leading theory posits that direction sensitivity could be computed at the level of dendrites and requires only excitatory stimuli, however little experimental support for this theory exists. Other theories disagree and propose that directional sensitivity requires an interaction between excitation and inhibition. We set out to investigate this question by using focal application of neurotransmitter to small segments of dendrites on hippocampal neurons. We show experimentally that, in contrary to the first theory, dendrites exhibit only minimal sensitivity to the temporal and the spatial order of activation of their excitatory inputs alone. By contrast, the spatial and the temporal order of synaptic activation become crucial if both excitatory and inhibitory neurons are activated concurrently. This E/I coupling then enables neurons to become directionally sensitive to the activation of their synaptic inputs. Individual branches on the neuron behave as independent units performing this direction sensitivity task, allowing parallel computation of

direction sensitivity that is combined at the soma to produce the final output. These experiments are the first demonstration in vitro that a careful coupling of excitatory and inhibitory synaptic activation can result in direction sensitivity of individual neurons.

INTRODUCTION

In many instances in the brain, individual neurons differ in their output depending on the temporal order of certain sensory events – for instance, the retinal ganglion cells exhibit sensitivity of to the direction of motion of light on the retina (Taylor, He et al. 2000; Euler, Detwiler et al. 2002; Fried, Munch et al. 2002), simple cells in the visual cortex display similar sensitivity to the direction of light stimulus (Borg-Graham, Monier et al. 1998; Anderson, Binzegger et al. 1999; Priebe and Ferster 2005), hippocampal place cells are often sensitive to the direction of the rat's movement on a linear track (Wilson and McNaughton 1993; Frank, Brown et al. 2001), and, finally, neurons in the barrel cortex can discriminate the texture of the surface during rat whisking, based on different temporal patterns of activation of their inputs (Jones, Lee et al. 2004). Although these computations are ubiquitous, it is unknown to what extent they can be mediated by individual cells, and to what extent they require encoding by a population of neurons.

A number of competing theories for how direction sensitivity could be computed at individual neurons have been proposed. Foremost, the oldest theory proposed by Rall (Rall 1964) required only the activation of excitatory inputs. Under this theory, the arrival of excitatory signals from more distal regions of dendrites is delayed with respect to the arrival of excitatory signal from more proximal regions because of dendritic filtering. Sequential activation of synapses from the distal region progressing toward the soma would then result in an approximately concurrent arrival of the signals at the soma, resulting in signal summation, whereas activation in the opposite direction would fail to summate since the signals would be more spread out temporally, and the signal from the proximal region would

decay significantly by the time the signal from the more distal region would arrive. Although attractive, there is currently little evidence supporting this model (Anderson, Binzegger et al. 1999; Euler, Detwiler et al. 2002). A competing theory has been proposed, which required activation of both excitatory and inhibitory inputs (Koch, Poggio et al. 1983). According to this theory, during a movement in the preferred direction, excitation is always closer to the cell body relative to inhibition, rendering inhibition ineffective and resulting in a strong excitatory summation in the soma. By contrast, during the movement in the null direction, inhibition would lie "on the path" of excitation toward the soma, effectively shunting it and thus preventing the neuron from responding. Simulations showed that such arrangement of synaptic activation, that is, inhibition always occurring more distally during movement in the preferred direction, and more proximally during movement in the null direction, would indeed cause a directionally sensitive response of the dendrite (Poggio and Koch 1987). Recently, Taylor et al. (Taylor and Vaney 2002) showed, using intracellular recording from direction-selective retinal ganglion cells, that indeed such asymmetry in the inhibition exists, but these results are debatable (Taylor, He et al. 2000; Borg-Graham 2001; Fried, Munch et al. 2002). Furthermore, even though such mechanism has been found feasible by simulating the effects of excitation and inhibition on the somatic firing, an experimental verification of the plausibility of this hypothesis has been lacking ever since its initial conception. Clearly, a detailed experimental study of the spatio-temporal interaction between excitatory and inhibitory inputs on a dendrite is required to verify the plausibility of any such theory. We propose that, by contrast to the theory of Koch et al. (Poggio and Koch 1987), which requires a spatially segregated activation of excitation and inhibition on the dendrite (such that inhibition always occurs more distally with respect to excitation during movement in the preferred direction, and proximally during movement in the null direction), concurrent activation of excitation and inhibition moving in either direction is sufficient to result in a strong directional selectivity. We propose and experimentally show that if both excitatory and inhibitory synapses are activated concurrently and locally within a small dendritic segment, and the location of this activated segment is moved either centripetally or centrifugally, strong direction selectivity will result.

Development of high spatial specificity iontophoresis technique and the ability to control the movement of the iontophoretic electrode by visual guidance enabled us to investigate the spatio-temporal interactions between excitatory and inhibitory synapses on the dendritic tree directly (Liu 2004). Here, we have studied the spatio-temporal interactions between excitatory-excitatory and excitatory-inhibitory synapses on the dendrites, and for the first time directly measured the effects of a sweeping activation of excitation and inhibition on the modulation of the cell's depolarization and firing rate.

RESULTS

To investigate the interaction between excitation and inhibition on the dendrites, we first investigated the impact of the relative timing of activation of two excitatory synapses on the depolarization and firing of the postsynaptic cell (Fig. 1a). We found that, as long as the synaptic currents were similar in their timecourse, their temporal interaction was perfectly symmetric. Thus, judging from the output, the cell was incapable of discriminating the particular order of activation of its excitatory inputs, whether in the measure of the peak magnitude of the EPSP, or the number of action potentials fired. (The interaction could be made asymmetric if the individual synaptic currents had different time course, favoring the arrival of the signal with longer decay time before the signal with a shorter decay time; however, for identical synaptic inputs, the interaction was perfectly symmetrical). However, when excitation was coupled to inhibition, a strong temporal asymmetry in the response resulted (Fig. 1b), preferring the arrival of inhibition before excitation. The timecourse of this asymmetry was determined by the timecourse of the $GABA_A$ receptor inhibitory current (Fig. 1b, red superimposed). Thus, although the dendrite could not distinguish the relative order of activation of two excitatory inputs, it readily distinguished the order of activation of an excitatory and an inhibitory connection.

We next turned to study the spatial aspect of the E-I interaction. To do this, we kept the location of the inhibitory electrode fixed and varied the location of the excitatory

electrode along the dendrite. We then tested for the ability of the inhibition to shunt the depolarizing effects of excitation on the somatic potential (Fig. 2a). To measure the degree of this shunting inhibition, we compared the depolarization evoked by the simultaneous arrival of excitation and inhibition against the linear sum of the responses elicited by excitation and inhibition alone. This gave us a measure of the effectiveness of inhibition to block out excitation. In agreement with theoretical predictions (Koch, Poggio et al. 1983), we found that inhibition located more distally to excitation had almost no impact on the excitatory efficacy, however, inhibitory synapses "on path" between excitation and the soma had a significant shunting effect. To characterize the effects of the location of inhibition on excitation more completely, we recorded a spatial "map" of the degree of inhibitory shunting on excitatory efficacy at different positions along the dendrite (Fig. 2b). The obtained spatial map and the curve predicted from theory matched closely. We also found that the sigmoidal spatial interaction function was localized to individual dendritic branches. Thus, the effects of inhibition were local and had no effects on excitation in a neighboring branch (Fig. 2b; lower panel). This independent processing of E/I activation by individual dendritic branches is akin to the independent processing of purely excitatory signals by individual dendritic branches predicted by modeling studies (Polsky, Mel et al. 2004).

Cable theory predicts that the degree of sigmoidity of the spatial interaction function of excitation and inhibition should depend on the degree of cable filtering at the dendrite, and on the strength of inhibition. Thus, for electrotonically compact cables, the spatial interaction function should appear nearly flat, and its sigmoidity and asymmetry should almost vanish (Fig. 2c). On the other hand, strong compartmentalization of the dendrite and poor electrotonic interaction between individual compartments should enhance the spatial asymmetry and sigmoidity. A similar effect would be predicted for a relatively weak inhibition (Fig. 2d). If the total inhibitory conductance is only a fraction of the total dendritic conductance (G_{SC} for semi-infinite cable in Fig. 2d), the spatial interaction map becomes more flattened and the effect disappears.

A crucial prediction of the spatiotemporal asymmetry shown in Figs.1-2 is that it should make dendrites capable of discriminating different directions of activation of their inputs. If inhibition arrives in the region proximal to the soma, it should effectively shunt any excitation that will occur concurrently, or within a short time interval afterwards (~40 ms, Fig. 1) in a more distal region. However, it will not affect excitation arriving in a more proximal region, nor excitation occurring in a more distal region prior to inhibition. As a consequence, then, the dendrite should be able to selectively respond to concurrent excitation and inhibition moving in the orthodromic direction (distal to proximal) and effectively filter out excitation and inhibition moving in the opposite antidromic direction (proximal to distal). To test this prediction, we stimulated the dendritic trunk with concurrent moving excitation and inhibition both in the orthodromic and antidromic direction and recorded the evoked somatic potential (Fig. 3a). Fig. 3a (bottom left) shows the response to stimulation of a linear dendritic segment by a moving sequence of 9 ejections of glutamate alone (Glut), GABA alone (GABA), the expected linear sum (Sum), or both glutamate and GABA (Glut+GABA), in the direction toward (blue) or away (red) from the cell. The effects on the timecourse of somatic depolarization were minimal for glutamate or GABA application alone, applied in either direction. However, centripetal stimulation produced robustly ~60% greater somatic depolarization than the equivalent stimulation in the centrifugal direction, if both glutamate and GABA were applied simultaneously. Importantly, the somatic response evoked by excitation moving in either direction alone failed to produce an observable difference (Fig. 3b; middle panel). Hence, dendrites could not distinguish the sequence of activation of excitatory inputs alone, but if excitation was coupled to inhibition, they could act as directional classifiers.

Since the degree of excitatory shunting by inhibition depends on the degree of overlap between the timecourse of excitation and (nearby or more proximal) inhibition (Fig. 1b), the degree of shunting during antidromic stimulation should also depend on the velocity of synaptic stimulation, since proximal inhibitory inputs would shunt distal excitation only if it occurs within the short ~50 ms span of the inhibitory timecourse. Thus, faster directional stimuli should produce more shunting than slower ones, and should be easier to distinguish.

We varied the velocity of the electrode movement along the dendritic segment, and changed the intervals between the stimulating pulses to adjust for this change in velocity, ensuring that stimuli would be delivered at approximately similar locations (Fig. 3b). We confirmed that the attenuation of the average response $\overline{V}_{out} / \overline{V}_{in}$ to stimulation in different directions depended strongly on the stimulation velocity (Fig. 3b, right). The magnitude of the cellular response was influenced by the rapidity of sequential activation, and could therefore be used for encoding of this important physical attribute of activity.

We wanted to further delineate the relative importance of excitation and inhibition on the dendritic sensitivity to the direction of synaptic firing. In particular, is it the sequential activation of excitatory synapses or of the inhibitory synapses that results in directional selectivity of the dendrite? To address this question, we simulated the effects of antidromic and orthodromic sequential stimulation of either excitatory or inhibitory events in the presence of random background synaptic noise of the other type (Fig. 4a). In the presence of random excitatory background and sweeping inhibition, the somatic response FERENCE_TYPE><REFNUM>1ity to the direction of stimulation (Fig. 4a; middle). By contrast, sweeping excitation in the presence of random inhibitory firing had no effect on the mean somatic response in either direction (Fig. 4a; right). Thus, directional selectivity is achieved because of sequential firing of inhibitory but not excitatory connections. Thus, the spatiotemporal pattern of activation of dendritic inhibitory synapses appears to be significantly more important in determining the cellular response than the spatiotemporal pattern of activation of excitatory synapses.

DISCUSSION

Our experiments show that dendrites are indeed capable of directionally selective responses mediated by sequential activation of their inhibitory inputs. However, one matter is to show that neurons are *capable* of computing direction selectivity via inhibition, and another matter is to show that they indeed *do* use this computation in real tasks. Most temporal sequences

in the cortex are encoded by sequential firing of individual neurons (for instance the sequential activation of hippocampal place cells during rat's movement). For this mechanism to be useful in the cortex at all, a simple mechanism must be present to translate sequential activation of neurons in a particular direction into sequential activation of synapses on the dendrite in an orthodromic or antidromic direction. The simplest way how this can be achieved is by organizing the synaptic connections in such fashion that neurons that fire first within a temporal sequence would synapse onto the most distal dendritic regions, and neurons late in the sequence would synapse onto the most proximal regions. For instance, encoding a sequence of activation of particular neurons corresponding to single digits to recognize a phone number could be achieved by an arrangement akin to the one shown in Fig. 4d. In this configuration, the neuron will preferentially respond to the sequence of digits 357920 or 542839, each encoded by a separate branch.

However, the arrangement in Fig. 4d would require plastic structural changes for memorization of a sequence of digits. Whether synaptic rearrangement at such scale occurs in the brain during learning is still largely unknown. However, it is possible that given some general anatomical considerations, even random connections in the brain might endow it with the capability to detect sequences. For instance, as long as closer neurons synapse onto more proximal dendritic regions and neurons further away connect to more distal dendritic regions (Fig. 4b), activation of (inhibitory!) neurons in the direction towards the target cell in the neural tissue will generally translate into orthodromic activation of the dendrite, and neuronal activation in the direction away from the cell will translate into antidromic activation sequence on the dendrite. This will in turn cause neurons to respond preferentially to the direction of activation of other cells toward them, but not away (Fig. 4b; right). The above anatomical assumption holds true for many excitatory recurrent connections and could be a general feature of brain wiring (Liu, Choi et al. 1999; Martina, Royer et al. 1999; Chklovskii 2004; Stepanyants, Tamas et al. 2004). Thus, on a two-dimensional surface of neurons, this rule might result in neurons responding to the activation of the neural tissue in the direction towards the cell, but selective suppression of

activation in the direction away from the cell (Fig. 4c). Sequence detection at this level might therefore be a natural consequence of the wiring in the brain.

Finally, proving conclusively that such computational tasks are used by dendrites in real sequence detection would involve visualizing the firing of individual synapses during various behavioral sequences, sequential recall, or directional stimulation, and showing that different sequences translate directly to different sequences of activation of excitatory and inhibitory synapses on the dendrite. The techniques for visualization of synaptic firing at such low level and high spatial and temporal resolution are not yet fully available, although hints of future possibilities appear (Miesenbock, De Angelis et al. 1998; Zakharenko, Zablow et al. 2001; Gandhi and Stevens 2003). It will be exciting to see this question resolved within the next years to come.

METHODS

Primary cultures of CA1-enriched hippocampal neurons were prepared from neonatal rats (P1) as described previously (Murnick, Dube et al. 2002). The age of the cultures ranged from 8 to 16 days *in vitro* (DIV). The composition of the extracellular solution for recording was (in mM): NaCl 153, KCl 2, $CaCl_2$ 1.2, $MgCl_2$ 1.2, glucose 10, Na_2HPO_4 0.95, NaH_2PO_4 0.2, and tetrodotoxin (TTX) 0.5 μM as required. Intracellular patch solution contained (in mM): K-gluconate 120, HEPES 10, NaCl 8, $CaCl_2$ 0.5, EGTA 5, MgATP 2, NaGTP 0.3, adjusted to pH 7.25 with KOH. All currents were filtered at 1 kHz and sampled at 20 kHz. Glutamate and GABA were delivered by fast focal iontophoresis as described previously (Koch, Poggio et al. 1983). Brief 1 ms pulses of glutamate (150mM) and GABA (200mM) were applied in isolated ejection events as well during sequential stimulation. The position of the iontophoretic microelectrodes was controlled by MP-285 micromanipulators (Sutter) and a custom software written in C++. Visual feedback of the electrode position was obtained by continuous imaging of the specimen by an SVC-1310 CCD camera (Epix). To activate synapses on the dendrite in sequence, the start and end points of a linear dendritic

segment were chosen on screen and fed into the software to define the start and end point for the manipulator sweeping movement. Movement velocity was adjusted by a command to the MP-285 controller delivered over a serial port. Electrode movement was synchronized with iontophoretic stimulation by a TTL pulse coinciding with the beginning of the movement and triggered stimulation.

APPENDIX

In the Appendix I derive the spatial interaction function between excitation and inhibition used to describe the data in Fig. 2. For the derivation I will consider an idealized case of an infinite cable with a point injection of excitatory current in the origin and investigate the effects of inhibitory conductance G_I at position L on the current flowing into either end of the cable, as this current will be proportional to the depolarization at the soma were it to be located at this end of the cable. With no inhibition, the membrane potential will be distributed according to the well-known exponential solution to the cable equation

$$V_x = V_0 e^{-|x|/\lambda} = \frac{I_E}{2G_{SC}} e^{-|x|/\lambda}$$

where $G_{SC} = \sqrt{G_A G_M}$ is the conductance of the semi-infinite cable and $\lambda = \sqrt{G_A / G_M}$ is its electrotonic length, with G_M and G_Λ being the usual membrane and axial conductances. What will be the effect of additive inhibitory conductance at position L on this distribution? In this case, the potential along the cable will follow the distribution:

$$\begin{aligned} V_x &= V_L e^{-x/\lambda} && \text{for } x>L \\ V_x &= V_0 \left(a e^{-x/\lambda} + b e^{x/\lambda} \right) && \text{for } L>x>0 \\ V_x &= V_0 e^{-x/\lambda} && \text{for } x<0 \end{aligned}$$

To solve for a, b, and V_0 note that at position L:

$$-\left.\frac{\partial V}{\partial x}\right|_L^- G_A = V_L\left(G_I + G_{SC}\right)$$

$$V_0/\lambda\left(ae^{-L/\lambda} - be^{L/\lambda}\right) = V_0\left(ae^{-L/\lambda} + be^{L/\lambda}\right)\left(G_I + G_{SC}\right)/G_A$$

$$ae^{-2L/\lambda}\left(1/\lambda - \left(G_I + G_{SC}\right)/G_A\right) = b\left(1/\lambda + \left(G_I + G_{SC}\right)/G_A\right)$$

$$ae^{-2L/\lambda}\left(G_{SC} - \left(G_I + G_{SC}\right)\right) = b\left(G_{SC} + \left(G_I + G_{SC}\right)\right)$$

$$b/a = -e^{-2L/\lambda}\frac{G_I}{2G_{SC} + G_I}$$

$$b/a = -\alpha e^{-2L/\lambda}$$

where α is defined as

$$\alpha = \frac{G_I}{2G_{SC} + G_I}$$

Because a + b = 1 (since V_x=V_0 at x = 0), we get $a = \frac{a}{a+b} = \frac{1}{1+b/a} = \frac{1}{1-\alpha e^{-2L/\lambda}}$.

We can then calculate the effective conductance $G_{SC}^{I=L}$ of the semi-infinite cable with inhibition G_I at position L:

$$G_{SC}^{I=L} = \frac{I_0}{V_0} = \frac{G_A\left.\frac{\delta V}{\delta x}\right|_0}{V_0} = \frac{G_A}{\lambda}\frac{V_0\left(a-b\right)}{V_0} = G_{SC}\left(a-b\right) = G_{SC}\frac{1-b/a}{1+b/a} = G_{SC}\frac{1+\alpha e^{-2L/\lambda}}{1-\alpha e^{-2L/\lambda}}$$

The voltage at x=0 will therefore be:

$$V_0^{I=L} = \frac{I_E}{G_{SC} + G_{SC}^{I=L}}$$

The attenuation of voltage at V_0 due to inhibition at L will then be

$$\frac{V_0^{I=L}}{V_0}=\frac{I_E/\left(G_{SC}+G_{SC}^{I=L}\right)}{I_E/\left(2G_{SC}\right)}=\frac{2G_{SC}}{G_{SC}+G_{SC}\dfrac{1+\alpha e^{-2L/\lambda}}{1-\alpha e^{-2L/\lambda}}}=\frac{2G_{SC}\left(1-\alpha e^{-2L/\lambda}\right)}{2G_{SC}}=1-\alpha e^{-2L/\lambda}$$

Thus, the current flowing into the cable contralateral to inhibition will be reduced by the factor of $1-\alpha e^{-2L/\lambda}$. This is the attenuation factor of the voltage at the soma by inhibition G_I, if inhibition is more distal than excitation. The attenuation of voltage at V_L will be

$$\frac{V_L^{I=L}}{V_L}=\frac{V_0^{I=L}\left(ae^{-L/\lambda}+be^{L/\lambda}\right)}{V_0e^{-L/\lambda}}=\frac{V_0^{I=L}}{V_0}\left(a-a\alpha\right)=\frac{V_0^{I=L}}{V_0}a\left(1-\alpha\right)=$$

$$=\frac{V_0^{I=L}}{V_0}\frac{1}{1+b/a}\left(1-\alpha\right)=\frac{V_0^{I=L}}{V_0}\frac{1-\alpha}{1-\alpha e^{-2L/\lambda}}=1-\alpha$$

and therefore the current flowing into the cable on the side of inhibition will be reduced by the factor of 1-α. This is equivalent to the attenuation factor of the somatic potential by inhibition G_I that lies more proximal than excitation.

Putting these together, the attenuation of the somatic potential by inhibition at a relative distance L to excitation (with positive L being distal to excitation) will be

$F=1-\alpha e^{-2L/\lambda}$ for L>0

$F=1-\alpha$ for L<0

Thus, inhibition introduced between excitation and the soma will attenuate the somatic response by the factor of 1-α. This factor depends on the strength of inhibition relative to the conductance of the semi-infinite cable G_{SC}, but is independent of the strength of excitatory current. By contrast, inhibition more distal to excitation has a tapering effect and wanes off exponentially with the distance between E and I relative to one half of the dendritic electrotonic length.

FIGURE LEGENDS

Figure.1. Temporal Characteristics of E/I Interactions.

A) (left) Two excitatory stimulating electrodes are positioned on a dendrite with ~60 μm separation. (right) The effects of timing of iontophoretic pulses on the magnitude of EPSP response recorded in the soma (with TTX; blue) and the number of action potentials (without TTX; red). B) (left) Excitatory and inhibitory electrodes positioned on the dendrite. (right) The effects of the relative timing of GABA and glutamate pulse on the magnitude of the recorded EPSP. In magenta is shown the superimposed timecourse of GABAR current.

Figure 2. E/I Interactions are spatially asymmetric and semi-local

A) The effects of electrode position on the summation of glutamate- and GABA-evoked synaptic potentials. Inhibition proximal to excitation or close to excitation causes shunting of the cellular response, whereas inhibition on the distal side of excitation has minimal effects. (bottom row) In red is the expected linear sum of the potentials evoked by glutamate and GABA alone, in black is the actual EPSP recorded when both glutamate and GABA are applied concurrently. B) Spatial map of the degree of shunting inhibition on different excitatory locations along the dendrite, computed as the ratio of the magnitude of the recorded response versus the magnitude of the expected sum of the E and I potentials. At each position, blue depicts the normalized response magnitude due to excitation alone and orange the relative magnitude due to simultaneous excitation and inhibition. Top panel shows a spatial interaction map along a single dendritic branch; bottom panel shows the effects of inhibition on excitatory potency at various locations along the same and neighboring branch. The effects of inhibition are restricted to the branch where it is located. C) Spatial effects of inhibition averaged over 5 dendritic maps. In red is the fit by a theoretical curve (see Appendix) D) The effects of different electrotonic length constants on the severity of spatial shunting by inhibition. The simulated 8 compartments comprised a fraction of one electrotonic length in powers of two. Electrotonically compact cables showed minimal asymmetry in the E-I interaction, whereas cables with significant filtering

showed maximal asymmetry. E) Spatial E-I interaction depends on the strength of inhibition relative to the conductance of the semi-infinite cable $G_{SC}=\sqrt{G_A G_M}$. In this formula, G_A is the axial conductance per unit length of the dendrite, and G_M is the membrane conductance per unit length of the dendrite.

Figure. 3. Cellular response depends on the direction of dendritic stimulation.

A) Excitatory (E) and inhibitory (I) electrodes positioned at identical locations on the dendrite and moved in synchrony toward and away from the cell soma (at velocity 200 μm/sec). (top panel) Iontophoretic stimulation (red) was synchronized with the electrode movement by means of a TTL pulse; electrode movement is characterized by the noise on the current trace recorded by a patch electrode in free solution (black). (bottom panels) Somatic response evoked by orthodromic (In) and antidromic (Out) stimulation by glutamate (blue), GABA (red), or both (black) compared to the linear sum (cyan). Movement in the Out direction is significantly more shunted than the movement in the In direction. B) Directional sensitivity requires inhibition. Outward stimulation produces only 59% of the response to inward stimulation when both E and I are present (top panel). However, excitation alone causes no difference in the cellular response to different directions of stimulation. C) Attenuation of the cellular response to outward versus inward direction of stimulation depends on the sweep velocity.

Figure 4. Various consequences of asymmetric E/I interaction

A) Dendritic sensitivity to the direction of stimulation requires sequential activation of inhibitory but not excitatory synapses. Simulations are based on a compartmental model of dendrite in Matlab. (Left) Concurrent activation of excitatory and inhibitory synapses in the antidromic direction causes only 59% response relative to orthodromic stimulation. (Middle) Sequential activation of inhibitory synapses in the presence of random Poisson firing of excitatory synapses causes 73% activation in the antidromic versus orthodromic

directions in the same compartmental model. (Right) However, sequential activation of excitatory synapses in the presence of random firing of inhibitory synapses causes no difference in the average cellular response. Thus, inhibition but not excitation confers directional selectivity to dendrites. B) Random cortical wiring with bias toward connections in more distal dendritic regions from distant neurons can map cellular activation sequence onto an activation sequence on the dendrite. Using this mapping, neurons could distinguish sequences of activation of other neurons. Simulated sequential activation of cell bodies toward the target cell produced 63% greater response than sequential activation away from the cell. C) This mechanism might cause neurons to become preferentially responsive to activation towards them on the cortical surface (red), and less responsive to activation away (blue). D) Topological configuration of inhibitory connections that might encode recognition of two sequences of numbers by a single cell.

FIGURES

Temporal Characteristics of E/I Interactions

E-E Interaction is Insensitive to Timing

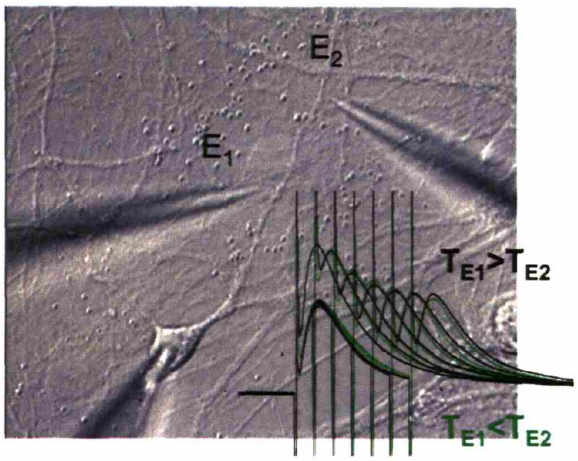

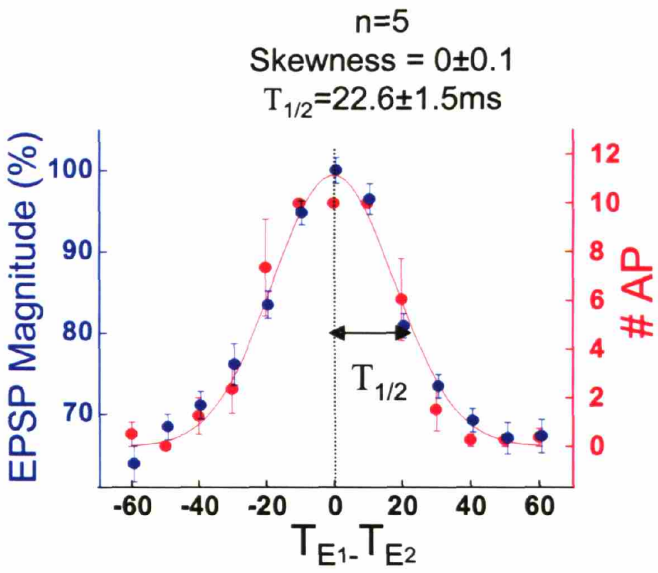

E-I Interaction is Sensitive to Timing

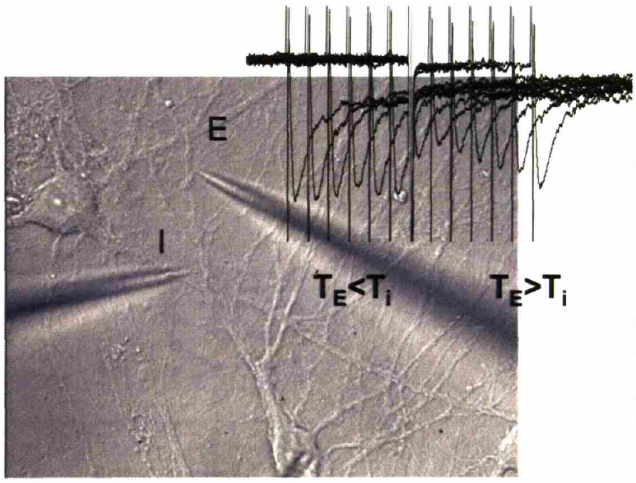

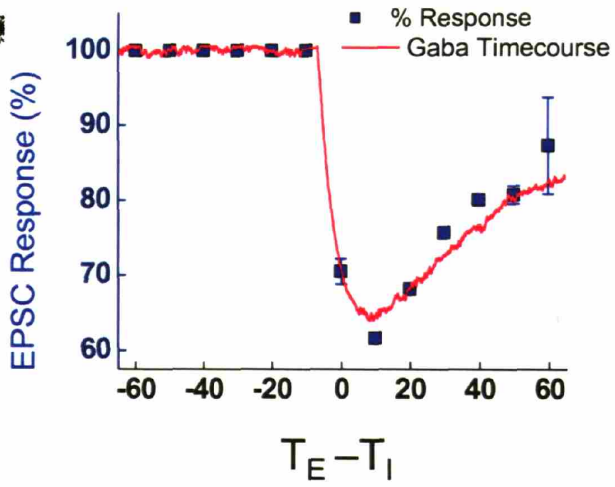

Fig. 1

Spatial Characteristics of E/I Interactions

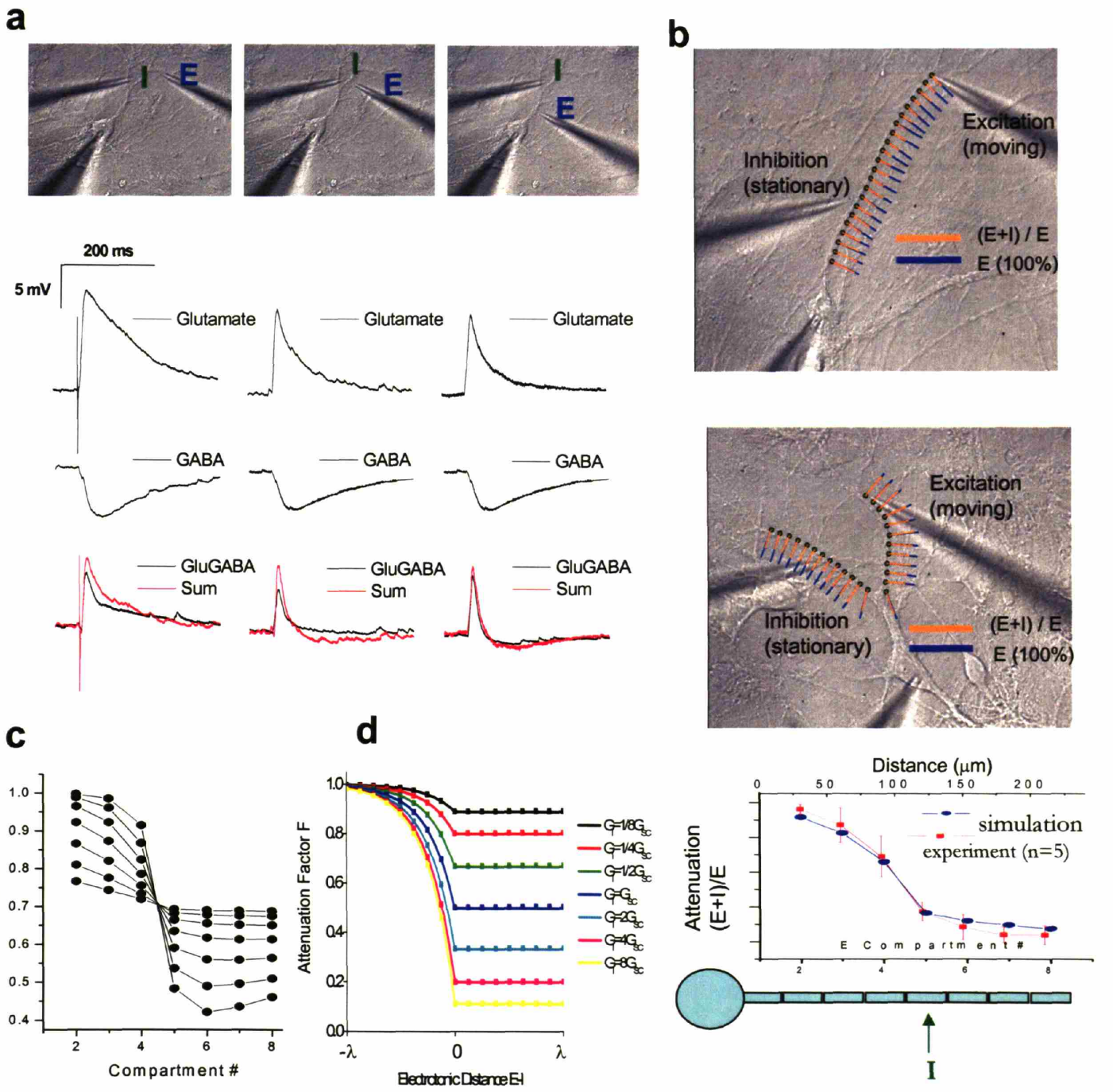

The effects of cable filtering on E/I interaction

The effects of the strength and position of on-path inhibition on E/I interaction

Fig. 2

a

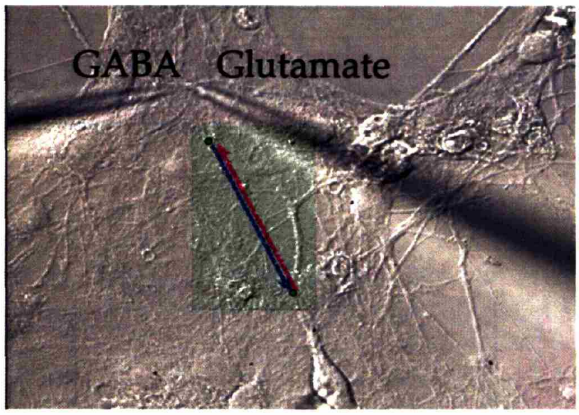

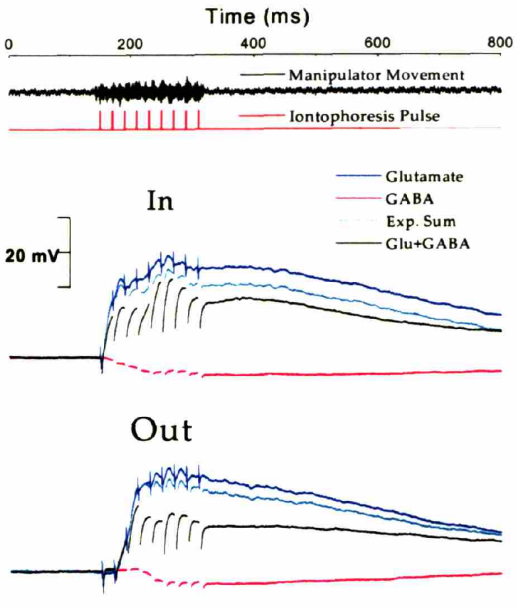

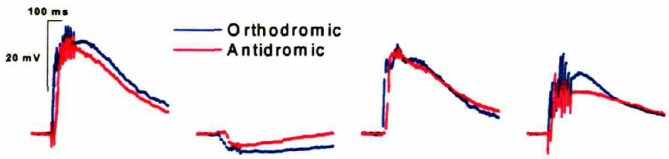

Glut GABA Sum Glut + GABA

b

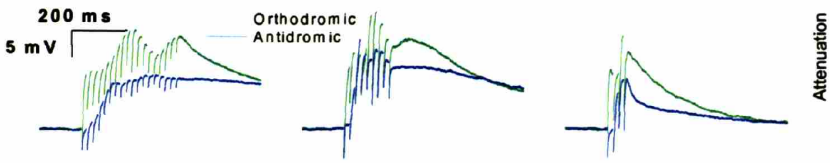

200 µm/sec 400 µm/sec 1000 µm/sec

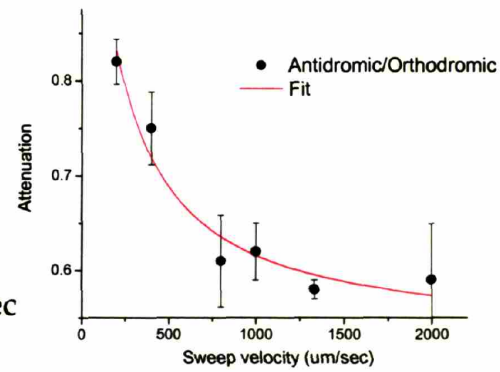

Fig. 3

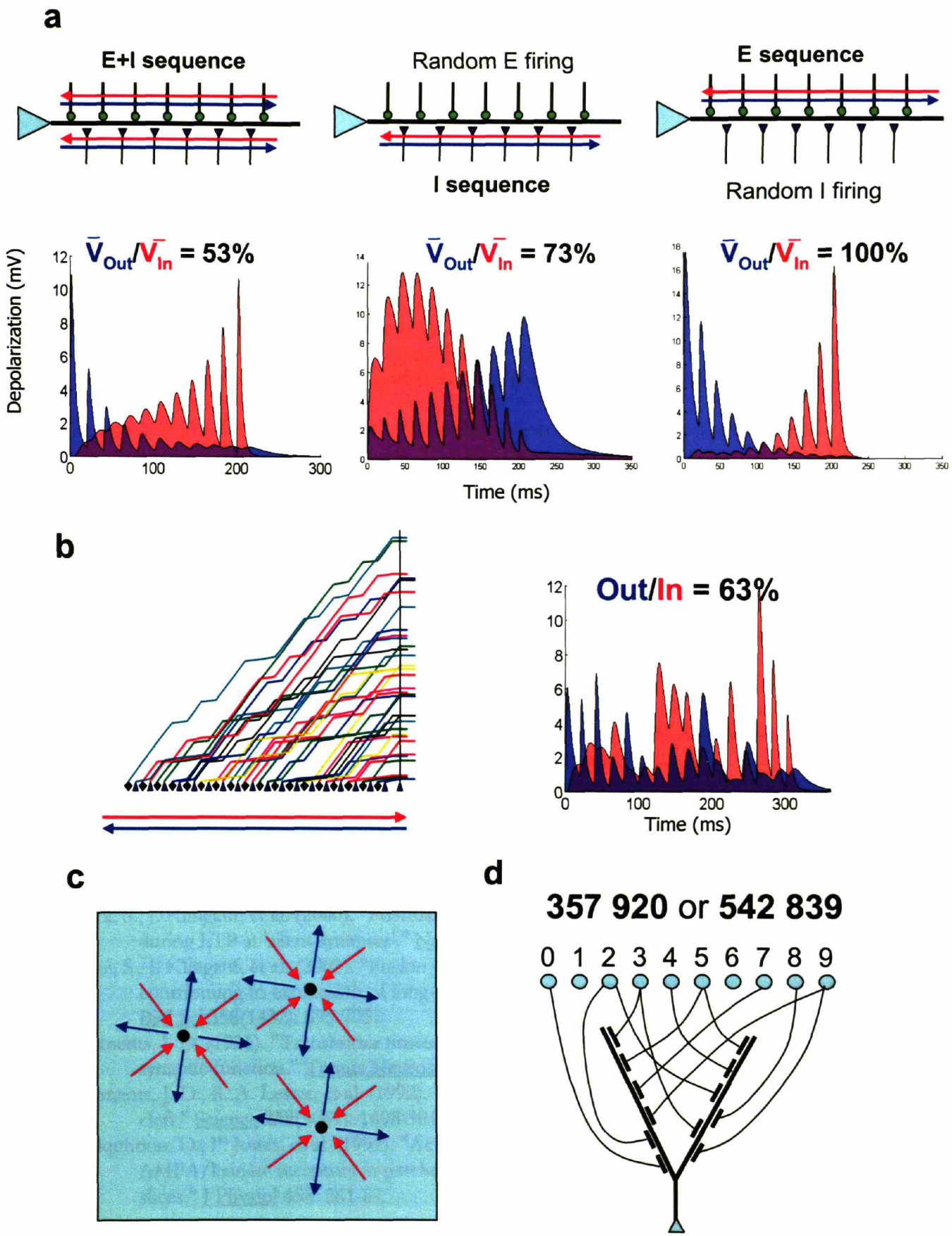
a
E+I sequence
Random E firing
E sequence
I sequence
Random I firing
Depolarization (mV)
$\bar{V}_{Out}/\bar{V}_{In}$ = 53%
$\bar{V}_{Out}/\bar{V}_{In}$ = 73%
$\bar{V}_{Out}/\bar{V}_{In}$ = 100%
Time (ms)
b
Out/In = 63%
Time (ms)
c
d
357 920 or 542 839
0 1 2 3 4 5 6 7 8 9

Fig. 4

IV. REFERENCES

Almers, W., L. J. Breckenridge, et al. (1991). "Millisecond studies of single membrane fusion events." Ann N Y Acad Sci **635**: 318-27.

Anderson, J. C., T. Binzegger, et al. (1999). "Dendritic asymmetry cannot account for directional responses of neurons in visual cortex." Nat Neurosci **2**(9): 820-4.

Asztely, F., G. Erdemli, et al. (1997). "Extrasynaptic glutamate spillover in the hippocampus: dependence on temperature and the role of active glutamate uptake." Neuron **18**(2): 281-93.

Barclay, J. W., T. J. Craig, et al. (2003). "Phosphorylation of Munc18 by protein kinase C regulates the kinetics of exocytosis." J Biol Chem **278**(12): 10538-45.

Bekkers, J. M., G. B. Richerson, et al. (1990). "Origin of variability in quantal size in cultured hippocampal neurons and hippocampal slices." Proc Natl Acad Sci U S A **87**(14): 5359-62.

Bolshakov, K. V. and S. L. Buldakova (2001). "Pharmacological analysis of the subunit composition of the AMPA receptor in hippocampal neurons." Neurosci Behav Physiol **31**(2): 219-25.

Borg-Graham, L. J. (2001). "The computation of directional selectivity in the retina occurs presynaptic to the ganglion cell." Nat Neurosci **4**(2): 176-83.

Borg-Graham, L. J., C. Monier, et al. (1998). "Visual input evokes transient and strong shunting inhibition in visual cortical neurons." Nature **393**(6683): 369-73.

Breckenridge, L. J. and W. Almers (1987). "Currents through the fusion pore that forms during exocytosis of a secretory vesicle." Nature **328**(6133): 814-7.

Chen, N., J. Ren, et al. (2001). "Changes in agonist concentration dependence that are a function of duration of exposure suggest N-methyl-D-aspartate receptor nonsaturation during synaptic stimulation." Mol Pharmacol **59**(2): 212-9.

Chklovskii, D. B. (2004). "Synaptic connectivity and neuronal morphology: two sides of the same coin." Neuron **43**(5): 609-17.

Choi, S., J. Klingauf, et al. (2000). "Postfusional regulation of cleft glutamate concentration during LTP at 'silent synapses'." Nat Neurosci **3**(4): 330-6.

Choi, S., J. Klingauf, et al. (2003). "Fusion pore modulation as a presynaptic mechanism contributing to expression of long-term potentiation." Philos Trans R Soc Lond B Biol Sci **358**(1432): 695-705.

Clements, J. D. (1996). "Transmitter timecourse in the synaptic cleft: its role in central synaptic function." Trends Neurosci **19**(5): 163-71.

Clements, J. D., R. A. Lester, et al. (1992). "The time course of glutamate in the synaptic cleft." Science **258**(5087): 1498-501.

Colquhoun, D., P. Jonas, et al. (1992). "Action of brief pulses of glutamate on AMPA/kainate receptors in patches from different neurones of rat hippocampal slices." J Physiol **458**: 261-87.

Colquhoun, D. and B. Sakmann (1985). "Fast events in single-channel currents activated by acetylcholine and its analogues at the frog muscle end-plate." J Physiol **369**: 501-57.
Cottrell, J. R., G. R. Dube, et al. (2000). "Distribution, density, and clustering of functional glutamate receptors before and after synaptogenesis in hippocampal neurons." J Neurophysiol **84**(3): 1573-87.
Dionne, V. E. (1981). "Acetylcholine receptor kinetics at slow fiber neuromuscular junctions." Fed Proc **40**(11): 2614-7.
Dionne, V. E. and C. F. Stevens (1975). "Voltage dependence of agonist effectiveness at the frog neuromuscular junction: resolution of a paradox." J Physiol **251**(2): 245-70.
Edmonds, B., A. J. Gibb, et al. (1995). "Mechanisms of activation of glutamate receptors and the time course of excitatory synaptic currents." Annu Rev Physiol **57**: 495-519.
Euler, T., P. B. Detwiler, et al. (2002). "Directionally selective calcium signals in dendrites of starburst amacrine cells." Nature **418**(6900): 845-52.
Fisher, R. J., J. Pevsner, et al. (2001). "Control of fusion pore dynamics during exocytosis by Munc18." Science **291**(5505): 875-8.
Forti, L., M. Bossi, et al. (1997). "Loose-patch recordings of single quanta at individual hippocampal synapses." Nature **388**(6645): 874-8.
Frank, L. M., E. N. Brown, et al. (2001). "A comparison of the firing properties of putative excitatory and inhibitory neurons from CA1 and the entorhinal cortex." J Neurophysiol **86**(4): 2029-40.
Franks, K. M., T. M. Bartol, Jr., et al. (2002). "A Monte Carlo model reveals independent signaling at central glutamatergic synapses." Biophys J **83**(5): 2333-48.
Franks, K. M., C. F. Stevens, et al. (2003). "Independent sources of quantal variability at single glutamatergic synapses." J Neurosci **23**(8): 3186-95.
Fried, S. I., T. A. Munch, et al. (2002). "Mechanisms and circuitry underlying directional selectivity in the retina." Nature **420**(6914): 411-4.
Gandhi, S. P. and C. F. Stevens (2003). "Three modes of synaptic vesicular recycling revealed by single-vesicle imaging." Nature **423**(6940): 607-13.
Gomperts, S. N., A. Rao, et al. (1998). "Postsynaptically silent synapses in single neuron cultures." Neuron **21**(6): 1443-51.
Grosskreutz, J., A. Zoerner, et al. (2003). "Kinetic properties of human AMPA-type glutamate receptors expressed in HEK293 cells." Eur J Neurosci **17**(6): 1173-8.
Grzywacz, N. M. and C. Koch (1987). "Functional properties of models for direction selectivity in the retina." Synapse **1**(5): 417-34.
Heckmann, M., J. Bufler, et al. (1996). "Kinetics of homomeric GluR6 glutamate receptor channels." Biophys J **71**(4): 1743-50.
Holmes, W. R. (1995). "Modeling the effect of glutamate diffusion and uptake on NMDA and non-NMDA receptor saturation." Biophys J **69**(5): 1734-47.
Isaac, J. T., R. A. Nicoll, et al. (1995). "Evidence for silent synapses: implications for the expression of LTP." Neuron **15**(2): 427-34.
Isaacson, J. S. and R. A. Nicoll (1993). "The uptake inhibitor L-trans-PDC enhances responses to glutamate but fails to alter the kinetics of excitatory synaptic currents in the hippocampus." J Neurophysiol **70**(5): 2187-91.

Ishikawa, T., Y. Sahara, et al. (2002). "A single packet of transmitter does not saturate postsynaptic glutamate receptors." Neuron **34**(4): 613-21.
Jonas, P., G. Major, et al. (1993). "Quantal components of unitary EPSCs at the mossy fibre synapse on CA3 pyramidal cells of rat hippocampus." J Physiol **472**: 615-63.
Jonas, P. and B. Sakmann (1992). "Glutamate receptor channels in isolated patches from CA1 and CA3 pyramidal cells of rat hippocampal slices." J Physiol **455**: 143-71.
Jones, L. M., S. Lee, et al. (2004). "Precise temporal responses in whisker trigeminal neurons." J Neurophysiol **92**(1): 665-8.
Jones, M. V., Y. Sahara, et al. (1998). "Defining affinity with the GABAA receptor." J Neurosci **18**(21): 8590-604.
Jones, M. V. and G. L. Westbrook (1995). "Desensitized states prolong GABAA channel responses to brief agonist pulses." Neuron **15**(1): 181-91.
Kenakin, T. (1997). Pharmacologic Analysis of Drug-Receptor Interaction. Philadelphia, Lippincott-Raven Publishers.
Kidd, F. L. and J. T. Isaac (2000). "Glutamate transport blockade has a differential effect on AMPA and NMDA receptor-mediated synaptic transmission in the developing barrel cortex." Neuropharmacology **39**(5): 725-32.
Klyachko, V. A. and M. B. Jackson (2002). "Capacitance steps and fusion pores of small and large-dense-core vesicles in nerve terminals." Nature **418**(6893): 89-92.
Koch, C., T. Poggio, et al. (1983). "Nonlinear interactions in a dendritic tree: localization, timing, and role in information processing." Proc Natl Acad Sci U S A **80**(9): 2799-802.
Krupa, B. and G. Liu (2004). "Does the fusion pore contribute to synaptic plasticity?" Trends in Neurosciences **27**(2): 62-66.
Kullmann, D. M., G. Erdemli, et al. (1996). "LTP of AMPA and NMDA receptor-mediated signals: evidence for presynaptic expression and extrasynaptic glutamate spill-over." Neuron **17**(3): 461-74.
Leranth, C., Z. Szeidemann, et al. (1996). "AMPA receptors in the rat and primate hippocampus: a possible absence of GluR2/3 subunits in most interneurons." Neuroscience **70**(3): 631-52.
Liao, D., N. A. Hessler, et al. (1995). "Activation of postsynaptically silent synapses during pairing-induced LTP in CA1 region of hippocampal slice." Nature **375**(6530): 400-4.
Liu, G. (2003). "Presynaptic control of quantal size: kinetic mechanisms and implications for synaptic transmission and plasticity." Curr Opin Neurobiol **13**(3): 324-31.
Liu, G. (2004). "Local structural balance and functional interaction of excitatory and inhibitory synapses in hippocampal dendrites." Nat Neurosci **7**(4): 373-9.
Liu, G., S. Choi, et al. (1999). "Variability of neurotransmitter concentration and nonsaturation of postsynaptic AMPA receptors at synapses in hippocampal cultures and slices." Neuron **22**(2): 395-409.
Liu, G. and R. W. Tsien (1995). "Properties of synaptic transmission at single hippocampal synaptic boutons." Nature **375**(6530): 404-8.
Mainen, Z. F., R. Malinow, et al. (1999). "Synaptic calcium transients in single spines indicate that NMDA receptors are not saturated." Nature **399**(6732): 151-5.

Malenka, R. C. and R. A. Nicoll (1997). "Silent synapses speak up." Neuron **19**(3): 473-6.
Malenka, R. C. and R. A. Nicoll (1999). "Long-term potentiation--a decade of progress?" Science **285**(5435): 1870-4.
Malinow, R., Z. F. Mainen, et al. (2000). "LTP mechanisms: from silence to four-lane traffic." Curr Opin Neurobiol **10**(3): 352-7.
Martina, M., S. Royer, et al. (1999). "Physiological properties of central medial and central lateral amygdala neurons." J Neurophysiol **82**(4): 1843-54.
Matthews-Bellinger, J. and M. M. Salpeter (1978). "Distribution of acetylcholine receptors at frog neuromuscular junctions with a discussion of some physiological implications." J Physiol **279**: 197-213.
McAllister, A. K. and C. F. Stevens (2000). "Nonsaturation of AMPA and NMDA receptors at hippocampal synapses." Proc Natl Acad Sci U S A **97**(11): 6173-8.
Miesenbock, G., D. A. De Angelis, et al. (1998). "Visualizing secretion and synaptic transmission with pH-sensitive green fluorescent proteins." Nature **394**(6689): 192-5.
Min, M. Y., D. A. Rusakov, et al. (1998). "Activation of AMPA, kainate, and metabotropic receptors at hippocampal mossy fiber synapses: role of glutamate diffusion." Neuron **21**(3): 561-70.
Murnick, J. G., G. Dube, et al. (2002). "High-resolution iontophoresis for single-synapse stimulation." Journal of Neuroscience Methods **116**(1): 65-75.
Oertner, T. G., B. L. Sabatini, et al. (2002). "Facilitation at single synapses probed with optical quantal analysis." Nat Neurosci **5**(7): 657-64.
Patneau, D. K. and M. L. Mayer (1990). "Structure-activity relationships for amino acid transmitter candidates acting at N-methyl-D-aspartate and quisqualate receptors." J Neurosci **10**(7): 2385-99.
Perkel, D. J. and R. A. Nicoll (1993). "Evidence for all-or-none regulation of neurotransmitter release: implications for long-term potentiation." J Physiol **471**: 481-500.
Petralia, R. S., J. A. Esteban, et al. (1999). "Selective acquisition of AMPA receptors over postnatal development suggests a molecular basis for silent synapses." Nat Neurosci **2**(1): 31-6.
Poggio, T. and C. Koch (1987). "Synapses that compute motion." Sci Am **256**(5): 46-52.
Polsky, A., B. W. Mel, et al. (2004). "Computational subunits in thin dendrites of pyramidal cells." Nat Neurosci **7**(6): 621-7.
Priebe, N. J. and D. Ferster (2005). "Direction selectivity of excitation and inhibition in simple cells of the cat primary visual cortex." Neuron **45**(1): 133-45.
Rall, W. (1964). Theoretical Significance of dendritic trees for neuronal input-output relations. Neural Theory and Modeling. R. Reiss. Standford, Stanford Univ. Press: 73-97.
Renger, J. J., C. Egles, et al. (2001). "A developmental switch in neurotransmitter flux enhances synaptic efficacy by affecting AMPA receptor activation." Neuron **29**(2): 469-84.
Rizo, J. and T. C. Sudhof (2002). "Snares and Munc18 in synaptic vesicle fusion." Nat Rev Neurosci **3**(8): 641-53.

Sakmann, B. and E. Neher (1995). Single-Channel Recording. New York, Plenum Press.
Scepek, S., J. R. Coorssen, et al. (1998). "Fusion pore expansion in horse eosinophils is modulated by Ca2+ and protein kinase C via distinct mechanisms." Embo J **17**(15): 4340-5.
Siegel, S. J., W. G. Janssen, et al. (1995). "Distribution of the excitatory amino acid receptor subunits GluR2(4) in monkey hippocampus and colocalization with subunits GluR5-7 and NMDAR1." J Neurosci **15**(4): 2707-19.
Stepanyants, A., G. Tamas, et al. (2004). "Class-specific features of neuronal wiring." Neuron **43**(2): 251-9.
Stevens, C. F. (2003). "Neurotransmitter release at central synapses." Neuron **40**(2): 381-8.
Stiles, J. R., D. Van Helden, et al. (1996). "Miniature endplate current rise times less than 100 microseconds from improved dual recordings can be modeled with passive acetylcholine diffusion from a synaptic vesicle." Proc Natl Acad Sci U S A **93**(12): 5747-52.
Taylor, W. R., S. He, et al. (2000). "Dendritic computation of direction selectivity by retinal ganglion cells." Science **289**(5488): 2347-50.
Taylor, W. R. and D. I. Vaney (2002). "Diverse synaptic mechanisms generate direction selectivity in the rabbit retina." J Neurosci **22**(17): 7712-20.
Tong, G. and C. E. Jahr (1994). "Block of glutamate transporters potentiates postsynaptic excitation." Neuron **13**(5): 1195-203.
Tong, G. and C. E. Jahr (1994). "Multivesicular release from excitatory synapses of cultured hippocampal neurons." Neuron **12**(1): 51-9.
Trussell, L. O., L. L. Thio, et al. (1988). "Rapid desensitization of glutamate receptors in vertebrate central neurons." Proc Natl Acad Sci U S A **85**(12): 4562-6.
Wilson, M. A. and B. L. McNaughton (1993). "Dynamics of the hippocampal ensemble code for space." Science **261**(5124): 1055-8.
Zakharenko, S. S., L. Zablow, et al. (2001). "Visualization of changes in presynaptic function during long-term synaptic plasticity." Nat Neurosci **4**(7): 711-7.
Zakharenko, S. S., L. Zablow, et al. (2002). "Altered presynaptic vesicle release and cycling during mGluR-dependent LTD." Neuron **35**(6): 1099-110.
Zhou, Q., T. A. Verdoorn, et al. (1998). "Alcohols potentiate the function of 5-HT3 receptor-channels on NCB-20 neuroblastoma cells by favouring and stabilizing the open channel state." J Physiol **507**(Pt 2): 335-52.
Zucker, R. S. (1996). "Exocytosis: a molecular and physiological perspective." Neuron **17**(6): 1049-55.